Original Research

Development of a Computed Tomography-Based Radiomics Model for Risk Stratification of Airflow Obstruction Progression

Suyin Huang, MD[1,2*] Fan Wu, MD, PhD[1*] Yanzhen Chen, MD[3] Kunning Zhou, MD[1] Zhishan Deng, MD, PhD[1] Qi Wan, MD[1] Gaoying Tang, MD[1] Ping Wang, MD[3] Qian Pang, MD[3] Kai Yang, MD[4] Cuiqiong Dai, MD[1] Lifei Lu, MD[1] Xiaohui Wu, MD[1] Fangyan Wu, MD[1] Changli Yang, MD[5] Shengtang Chen, MD[5] Yongqing Huang, MD[6] Shuqing Yu, MD[7] Yu Deng, MD, PhD[8] Pixin Ran, MD, PhD[1,2**] Yumin Zhou, MD, PhD[1,2**]

[1]State Key Laboratory of Respiratory Disease and National Clinical Research Center for Respiratory Disease and National Center for Respiratory Medicine and Guangzhou Institute of Respiratory Health, First Affiliated Hospital of Guangzhou Medical University, Guangzhou Medical University, Guangzhou, China

[2]Guangzhou National Laboratory, Guangzhou, China

[3]Hangzhou Smart Intelligent Co. Ltd., Hangzhou, China

[4]Department of Pulmonary and Critical Care Medicine, Shenzhen Institute of Respiratory Diseases, Shenzhen People's Hospital, Shenzhen, China

[5]Wengyuan County People's Hospital, Shaoguan, China

[6]Lianping County People's Hospital, Heyuan, China

[7]Lianping County Second People's Hospital, Heyuan, China

[8]Department of Radiology, First Affiliated Hospital of Guangzhou Medical University, Guangzhou, China

**Contributed equally to this work*
***Co-senior authors*

Address correspondence to:
Yumin Zhou, MD, PhD
151 Yanjiang Xi Road,
510120
Guangzhou, China
Email: zhouyumin410@126.com

Running Head: **CT Radiomics and Airflow Obstruction Development**

Keywords**:** airflow obstruction; chronic obstructive pulmonary disease; chest CT; radiomics; machine learning

Pre-Proof

Copyright *Chronic Obstructive Pulmonary Diseases: Journal of the COPD Foundation* ©2026
Published online November 24, 2026 https://doi.org/10.15326/jcopdf.2026.0850

***Abbreviations*:**

***Funding Support*:** This work was supported by the National Natural Science Foundation of China (82570065 and 82472076), and the Foundation of Guangzhou National Laboratory (SRPG22-016 and SRPG22-018), the Clinical and Epidemiological Research Project of State Key Laboratory of Respiratory Disease (SKLRD-L-202402), the Major Clinical Research Project of Guangzhou Medical University's Scientific Research Capability Improvement Plan (GMUCR2024-01012), and the Noncommunicable Chronic Diseases-National Science and Technology Major Project (2024ZD0528401).

Date of Acceptance: October 30, 2026 | ***Published Online Date***: November 24, 2026

Citation: Huang S, Wu F, Chen Y, et al. Development of a computed tomography-based radiomics model for risk stratification of airflow obstruction progression. *Chronic Obstr Pulm Dis.* 2026; Published online November 24, 2026.
https://doi.org/10.15326/jcopdf.2026.0850

This article has an online supplement.

Pre-Proof

Abstract

Objectives: We developed a machine learning model integrating clinical and computed tomography (CT) radiomics features to stratify the risk of airflow obstruction (AO) development for early prevention.

Methods: Participants without AO at baseline from the ECOPD study were randomly assigned into training (70.0%) and testing (30.0%) datasets. Spirometry-defined AO was defined as postbronchodilator forced expiratory volume in 1 second (FEV_1)/ forced vital capacity <0.70. CT radiomics features were selected using Least Absolute Shrinkage and Selection Operator regression to generate radscore. The combined model incorporating the clinical model (clinical variables) and the radiomic model (radscore) effectively stratified participants into low-risk and high-risk groups for AO development at the third-year follow-up using the maximum Youden index-determined cutoff from the training dataset. Model performance was assessed by the area under the receiver operating characteristic curve (AUC).

Results: The training and testing datasets showed AO development proportions of 10.5% (n=69) and 9.6% (n=27). There was no statistical difference in AUCs between the combined (0.807), clinical (0.777) and radiomic (0.774) models in the testing dataset. In the combined model, high-risk participants had higher risk of AO development (18.3% vs. 3.1%; adjusted odds ratio 2.49, P= 0.181) and accelerated annual lung function decline (postbronchodilator FEV_1: 32±6 mL/year vs. 19±5 mL/year, adjusted P=0.047) than low-risk participants.

Conclusion: The combined model integrating clinical and CT radiomic features exhibited slightly better predictive performance, facilitating precise and individualized risk stratification for AO development. It may guide proactive management of high-risk individuals while sparing low-risk individuals from frequent spirometry screening, thereby optimizing the use of limited

Pre-Proof

Copyright *Chronic Obstructive Pulmonary Diseases: Journal of the COPD Foundation* ©2026
Published online November 24, 2026 https://doi.org/10.15326/jcopdf.2026.0850

healthcare resources.

Pre-Proof

Copyright *Chronic Obstructive Pulmonary Diseases: Journal of the COPD Foundation* ©2026
Published online November 24, 2026 https://doi.org/10.15326/jcopdf.2026.0850

Introduction

Chronic obstructive pulmonary disease (COPD) is a heterogeneous disease characterized by chronic respiratory symptoms and persistent airflow obstruction [1]. Owing to its high global prevalence, COPD is the third leading cause of death worldwide, imposing a substantial economic burden [2]. Pharmacological therapies for COPD alleviate respiratory symptoms, improve lung function, and reduce acute exacerbation frequency, yet they fail to reverse pulmonary structural damage or effectively delay disease progression [3-4]. Recently, experts have proposed that the early identification of COPD enables timely initiation of precision interventions, which may mitigate or halt disease progression [5-6].

Studies have attempted to identify populations at risk of COPD development based on demographic characteristics, COPD-related risk factors, and spirometry parameters [7-8]. However, these models demonstrate limited predictive accuracy or remain confined to individual-level predictions without the potential for clinical translation. Emerging evidence suggests that individuals in the pre-COPD stage, prior to the manifestation of physiological airflow obstruction, already exhibit pathological changes, such as emphysema, reduced small airway number, and airway remodeling [9]. Computed tomography (CT) radiomics uses high-throughput computational methods to extract quantitative features from CT images [10]. This process converts imaging data into high-dimensional datasets capable of quantifying subtle spatial tissue patterns [11]. CT radiomics features have been integrated with clinical variables and quantitative CT parameters to classify COPD disease status and severity, with good predictive performance [12-14]. However, there is insufficient evidence to determine whether combining CT radiomics features with clinical variables improves the identification of individuals at elevated risk of airflow obstruction (AO) development.

Pre-Proof

Copyright *Chronic Obstructive Pulmonary Diseases: Journal of the COPD Foundation* ©2026
Published online November 24, 2026 https://doi.org/10.15326/jcopdf.2026.0850

To enable the early identification of high-risk populations for AO development, we integrated CT radiomics features and clinical variables to construct a model that could stratify the risk of developing AO. We hypothesize that this model will be useful to accurately stratify AO development risk, thereby providing a scientific basis for initiating tailored pre-COPD management strategies for different risk populations. To validate this hypothesis, we used data from participants without spirometry-defined AO at baseline from the Early Chronic Obstructive Pulmonary Disease (ECOPD) study, to develop and test a machine learning-based risk stratification model integrating CT radiomics features with clinical variables to predict AO development.

Materials and Methods

Study design and participants

The ECOPD study was a prospective, observational, multicenter, community-based study conducted in XXX from July 2019 to September 2024. The ECOPD study recruited participants from the communities in XXX. The ECOPD study was designed to enroll approximately 1000 participants without airflow obstruction and approximately 1000 participants with airflow obstruction. Participants were screened through a large COPD epidemiologic survey. According to the results of China's 2018 COPD prevalence survey, the estimated prevalence of airflow obstruction in people aged 40-80 is around 15% [15]. To enroll a similar number of participants without airflow obstruction and those with airflow obstruction, all screened participants with airflow obstruction were invited to participate in the ECOPD study. For participants without airflow obstruction, 1 of every 4 participants was invited to participate in the ECOPD study in the order of spirometry completion. The study protocol and design have been published [16]. The

Pre-Proof

Copyright *Chronic Obstructive Pulmonary Diseases: Journal of the COPD Foundation* ©2026
Published online November 24, 2026 https://doi.org/10.15326/jcopdf.2026.0850

ECOPD study received approval from the Ethics Committee of XXX (No. 2018-53), and all participants provided written informed consent. The inclusion and exclusion criteria for the ECOPD study are shown in the **Supplementary Methods**.

We included participants without spirometry-defined AO at baseline from the ECOPD study. All participants had complete baseline data, including the standard respiratory epidemiological questionnaires, pre- and postbronchodilator spirometry, and chest CT scans, in addition to 3-year follow-up spirometry data. The study flowchart is shown in **Supplementary Figure S1**. A total of 937 participants were included and randomly split into the training (n=656) and testing (n=281) datasets (7:3) for model development and validation. The age and male proportion of the participants in the training dataset and the testing dataset were comparable.

Questionnaires

This study collected demographic information, COPD-related risk factors, and chronic respiratory symptoms [17]. Questionnaire details are in the **Supplementary Methods**.

Spirometry

Pre- and postbronchodilator spirometry was performed by trained physicians using portable spirometers (CareFusion, Yorba Linda, CA, USA) in accordance with the American Thoracic Society and European Respiratory Society technical standards for equipment performance and quality control [18-19]. Details about the spirometry assessment are in the **Supplementary Methods**. Spirometry-defined AO was defined as postbronchodilator forced expiratory volume in 1 second (FEV_1)/forced vital capacity (FVC) <0.70 [1]. AO development was defined as postbronchodilator FEV_1/FVC ≥0.70 at baseline and postbronchodilator FEV_1/FVC <0.70 at the third-year follow-up.

CT image acquisition, segmentation, and preprocessing

Pre-Proof

Copyright *Chronic Obstructive Pulmonary Diseases: Journal of the COPD Foundation* ©2026
Published online November 24, 2026 https://doi.org/10.15326/jcopdf.2026.0850

All participants underwent inspiratory chest CT performed using the Siemens Definition AS Plus 128-slicers or United-imaging uCT 760 128-slicers (**Supplementary Table S1, Supplementary Table S2**). The CT images were segmented using AVIEW software (1.1.42.2001-win, Coreline Soft Co. Ltd.) followed by preprocessing. Details about CT image acquisition, segmentation, and preprocessing are in the **Supplementary Methods**.

Radiomics features extraction and selection

Using the PyRadiomics (version 3.0.1), 1,239 radiomics features were extracted from chest CT images in compliance with the Image Biomarker Standardization Initiative guidelines (**Figure 1**, **Supplementary Table S3**) [20]. Details about features extraction, Z-score normalization, dimensionality reduction, and features selection performed on the CT radiomics features are in the **Supplementary Methods**, **Supplementary Calculation formula**, and **Supplementary Table S4**. The radscore was calculated as a linear combination of the selected features weighted by their respective coefficients from the Least Absolute Shrinkage and Selection Operator (LASSO) regression analysis (**Supplementary Calculation formula**).

Model construction and evaluation

The clinical variables (age, sex, BMI, smoking status, and smoking index) have been consistently identified as factors closely related to COPD in previous research [1]. Based on significant clinical features ($P < 0.05$) identified by univariable logistic regression, the radscore, and their combination, we constructed clinical, radiomic, and combined models in accordance with the transparent reporting of a multivariable prediction model for individual prognosis or diagnosis (TRIPOD) statement [21]. We selected the optimal machine learning algorithm for model construction. Details about model construction are provided in **Supplementary Methods**. The performance of the three models was evaluated using the area under the receiver operating

Pre-Proof

Copyright *Chronic Obstructive Pulmonary Diseases: Journal of the COPD Foundation* ©2026
Published online November 24, 2026 https://doi.org/10.15326/jcopdf.2026.0850

characteristic (ROC) curve (AUC), accuracy, sensitivity, specificity, positive predictive value, negative predictive value, and F1 score. The AUC and its 95% confidence interval (CI) were calculated using the Clopper-Pearson method [22]. DeLong test was used to compare the AUC among the models [23]. The calibration curves were performed to evaluate the calibration of the models. Decision curve analysis was applied to evaluate the clinical practicability of the models. A machine learning-based classifier was developed to stratify the risk of AO development (**Figure 1**). The cutoff value determined by the maximum Youden index from the training dataset was used to categorize the participants into low-risk and high-risk groups [24]. A nomogram was developed to visualize the predictive outcomes of the combined model and to graphically assess the importance of each variable. Furthermore, we constructed a free, user-friendly web-based calculator to enhance the clinical utility of the combined model.

Statistical analysis

Baseline characteristics were compared using the independent samples t-test or Mann-Whitney U test for continuous variables, and the chi-square test or Fisher's exact test for categorical variables, as appropriate. Spearman's correlation test was used to assess the association of the radscore with postbronchodilator FEV_1/FVC at the third-year follow-up and the annualized change in postbronchodilator FEV_1/FVC. The machine learning model analysis was performed using the "glmnet", "caret", and "mlr3" packages for model development and evaluation, along with the "ggplot2" package for data visualization. ROC curve analysis was performed using the "pROC" package. Multivariable logistic regression was performed to evaluate the associations of different risk groups or the radscore with the risk of AO development at the third-year follow-up. Annual lung function decline was compared between the groups using random coefficient regression models, while differences in lung function between the groups across multiple visits

Pre-Proof

Copyright *Chronic Obstructive Pulmonary Diseases: Journal of the COPD Foundation* ©2026
Published online November 24, 2026 https://doi.org/10.15326/jcopdf.2026.0850

were assessed using mixed-effects models [25]. Random coefficient model was used to evaluate the association between the radscore and annual lung function decline. Details about random coefficient model are provided in **Supplementary Methods**. To evaluate the risk of AO development and lung function decline, we adjusted for age, sex, BMI, smoking status, smoking index, biomass exposure, occupational exposure, and family history of respiratory diseases. To evaluate lung function decline, additional adjustments were made for corresponding baseline lung function parameters. The independent associations of the radscore with the risk of AO development and annual lung function decline were evaluated after further adjusting for inspiratory LAA_{-950}, expiratory LAA_{-856}, and Pi 10. Since the training dataset was used for model development, we performed the sensitivity analysis in an independent dataset comprising participants with baseline postbronchodilator $FEV_1/FVC \geq$the lower limit of normal (LLN) to validate the risk stratification performance of the combined model. To minimize the potential impact of measurement variability, a sensitivity analysis was performed in participants with baseline postbronchodilator $FEV_1/FVC \geq 0.75$. Only participants with complete data were included in the study, and no imputation was performed for missing data. Two-sided $P<0.05$ was considered statistically significant. R (version 4.4.2) and SAS (version 9.4) software were used for the statistical analyses.

Results

Baseline characteristics

In the training dataset, 69 (10.5%) participants progressed to AO at the third-year follow-up, while 27 (9.6%) participants developed AO in the testing dataset (**Supplementary Figure S1**). The baseline characteristics of the participants are in **Table 1**. In both the training and testing

Pre-Proof

Copyright *Chronic Obstructive Pulmonary Diseases: Journal of the COPD Foundation* ©2026
Published online November 24, 2026 https://doi.org/10.15326/jcopdf.2026.0850

datasets, participants who progressed to AO were older, had higher proportion of males, lower BMI, and higher smoking proportion at baseline than those who did not progress to AO (all $P<0.05$).

Features extraction and selection

Figure 2 illustrates the radiomics features selection process. A total of 1,239 radiomics features were extracted from the inspiratory CT images and Z-score normalized. After removing highly correlated features and retaining those with minimal redundancy by maximum relevance minimum redundancy analysis, 20 features were preserved. LASSO regression further identified 9 features with non-zero coefficients (**Figure 2A, B**). These nine features were weighted by their respective coefficients to generate the radscore, which was calculated for each participant using the defined formula (**Figure 2C, Supplementary Calculation formula).** In the training and testing datasets, participants who progressed to AO exhibited significantly higher radscore than those who did not (all $P<0.05$) (**Table 1**). The radscore was negatively correlated with postbronchodilator FEV_1/FVC at the third-year follow-up, while being positively correlated with the annual change in postbronchodilator FEV_1/FVC over the three-year follow-up period (all $P<0.05$) (**Supplementary Table S5**). Higher radscore was associated with higher risk of AO development and faster decline in prebronchodilator FEV_1 after confounders adjustment (**Supplementary Table S6**). Additionally, age, sex, BMI, smoking status, smoking index, and the radscore demonstrated significant associations with AO development risk at the third-year follow-up in the training dataset (all $P<0.05$) (**Figure 2D**). Consequently, age, sex, BMI, smoking status, and smoking index were incorporated into the clinical model, and the radscore was used to build the radiomic model. The combined model integrated all of these variables.

Model construction and performance

Pre-Proof

Copyright *Chronic Obstructive Pulmonary Diseases: Journal of the COPD Foundation* ©2026
Published online November 24, 2026 https://doi.org/10.15326/jcopdf.2026.0850

Figure 2E-G and **Supplementary Table S7** demonstrate the performance of eight machine learning algorithms across different models in the training dataset. In the clinical, radiomic, and combined models, the logistic regression algorithm demonstrated better performance with the highest mean AUC among all evaluated algorithms. Therefore, logistic regression was selected for model development. The predicted probability formula for the combined model is provided in the **Supplementary Calculation formula**.

Figure 2H-I and **Table 2** illustrate the performance evaluation for constructing the AO development risk stratification model. According to Delong test, the AUC of the combined model was higher than that of the clinical model in the training dataset (AUC 0.807, 95%CI 0.757-0.856 vs. AUC 0.761, 95%CI 0.707-0.815; P=0.008), but there was no significant difference in the testing dataset (AUC 0.807, 95%CI 0.715-0.900 vs. AUC 0.777, 95%CI 0.688-0.865; P=0.226). Similarly, the combined model outperformed the radiomic model in the training (AUC 0.807, 95%CI 0.757-0.856 vs. AUC 0.785, 95%CI 0.731-0.839; P=0.559) and testing (AUC 0.807, 95%CI 0.715-0.900 vs. AUC 0.774, 95%CI 0.681-0.866; P=0.197) datasets, although the differences were not significant. In the testing dataset, the Brier scores for the clinical, radiomic, and combined models were 0.078, 0.081, and 0.076, respectively. The Brier score in each model had no statistically significant differences observed by Spiegelhalter's test (all $P > 0.05$). (**Supplementary Figure S2**). The decision curves for the clinical, radiomic, and combined models are presented in **Supplementary Figure S3**.

Model-predicted risk stratification of AO development and lung function decline

We determined the optimal thresholds for risk stratification of AO development using maximum Youden index in the training dataset of the clinical model (0.075), the radiomic model (0.113) and combined model (0.087). In the training and testing datasets of the combined model, the

Pre-Proof

Copyright *Chronic Obstructive Pulmonary Diseases: Journal of the COPD Foundation* ©2026
Published online November 24, 2026 https://doi.org/10.15326/jcopdf.2026.0850

high-risk group was significantly older and had a higher proportion of male individuals, lower BMI, higher smoking index, lower postbronchodilator FEV_1/FVC, and elevated radscore at baseline than the low-risk group (all P<0.05) (**Supplementary Table S8**). The combined model demonstrated distinct AO development in both the training (low-risk: 2.5% vs high-risk: 22.9%, **Figure 3A**) and testing (low-risk: 3.1% vs high-risk: 18.3%, **Figure 3B**) datasets. The combined model exhibited risk discrimination, with unadjusted odd ratio (OR) of 11.50 (95% CI 5.76-22.97, P<0.001) and 7.00 (95% CI 2.57-19.10, P<0.001) for the high- versus low-risk groups in the training and testing datasets, respectively (**Figure 3A-B**). After adjusting for covariates, the corresponding adjusted OR were 6.58 (95% CI 2.42-17.86, P<0.001) and 2.49 (95% CI 0.65-9.51, P=0.181) in the training and testing datasets, respectively (**Figure 3A-B**). The radiomic model also enabled risk stratification of AO development, with an adjusted OR of 3.78 (95% CI 1.35-10.62, P=0.012) in the testing dataset (**Supplementary Figure S4**). The high-risk group tended to have higher risk of AO development than the low-risk group in the testing dataset of the clinical model (**Supplementary Figure S5**). When using the LLN instead of the fixed ratio to define AO, the high-risk group had higher risk of AO development compared to the low-risk group after confounders adjustment in the combined model (**Supplementary Table S9**).

The annual rates of decline in prebronchodilator FEV_1 (31±3 mL/year vs. 16±3 mL/year, adjusted mean difference=13 mL/year, 95% CI 4-23 mL/year; P=0.005), postbronchodilator FEV_1 (36±3 mL/year vs. 24±3 mL/year, adjusted mean difference=9 mL/year, 95% CI -1 to 19 mL/year; P=0.078), and postbronchodilator FEV_1/FVC (0.5±0.1 %/year vs. -0.1±0.1 %/year, adjusted mean difference=0.5 %/year, 95% CI 0.2-0.8 %/year; P<0.001) were greater in the high-risk group than in the low-risk group in the training dataset of the combined model (**Figure 4A-C**). Similarly, high-risk group had more accelerated annual rate of decline in

Pre-Proof

Copyright *Chronic Obstructive Pulmonary Diseases: Journal of the COPD Foundation* ©2026
Published online November 24, 2026 https://doi.org/10.15326/jcopdf.2026.0850

prebronchodilator FEV_1 (adjusted mean difference=22 mL/year, 95% CI 7-38 mL/year; P=0.005), postbronchodilator FEV_1 (adjusted mean difference=16 mL/year, 95% CI 0-32 mL/year; P=0.047), and postbronchodilator FEV_1/FVC (adjusted mean difference=0.4 %/year, 95% CI: 0.0-0.8 %/year; P=0.053) than the low-risk group in the testing dataset of the combined model (**Figure 4D-F**). In both the radiomic and clinical models, the high-risk group demonstrated a trend toward faster annual lung function decline than the low-risk group in the testing dataset, although no statistically significant difference was observed in postbronchodilator FEV_1 and postbronchodilator FEV_1/FVC (**Supplementary Figure S6, Supplementary Figure S7**). When using the LLN instead of the fixed ratio to define AO, the high-risk group had faster lung function decline compared to the low-risk group after confounders adjustment in the combined model (**Supplementary Table S9**). Among participants with baseline postbronchodilator FEV_1/FVC ≥0.75, the high-risk group exhibited significantly faster rate of postbronchodilator FEV_1/FVC decline than the low-risk group after adjusting for confounders (**Supplementary Table S10**).

Web-based calculator

The combined model was converted into a nomogram (**Figure 5A**). A predicted risk probability of ≤0.087 indicated a low risk of spirometry-defined AO development, whereas a probability exceeding this threshold suggested a high risk. An online calculator based on the combined model was developed and is now operational on the platform (https://suyinhuang.shinyapps.io/COPD_Risk_Calculator/). **Figure 5B** shows an example of using the online calculator. By entering the values of the six required predictors for risk

Pre-Proof

Copyright *Chronic Obstructive Pulmonary Diseases: Journal of the COPD Foundation* ©2026
Published online November 24, 2026 https://doi.org/10.15326/jcopdf.2026.0850

stratification and clicking the "Calculate Risk" button, users can automatically obtain the risk stratification of AO development.

Discussion

In this study, we developed and validated a prediction model for stratifying the risk of spirometry-defined AO development by integrating CT radiomics features with clinical variables using machine learning algorithms. The combined model tended to perform better in the training and testing datasets compared with the models relying solely on either clinical variables or radiomics features, though the differences were not always statistically significant. Furthermore, individuals classified as high-risk by the combined model showed increased likelihood of developing AO at the third-year follow-up and exhibited accelerated lung function decline compared with the low-risk group.

To our knowledge, this study establishes the risk stratification prediction model for spirometry-defined AO development in community populations by integrating CT radiomics features with clinical variables. The model is applicable to individuals undergoing lung cancer screening or annual health check-ups, facilitating opportunistic case-finding identification and management. The model identifies high-risk individuals for early identification of COPD and enables timely initiation of intervention and management. The model also identifies low-risk populations to reduce unnecessary frequent spirometry screenings and optimize the allocation of limited medical resources. Previous artificial intelligence studies on COPD-related medical imaging have focused on improving model accuracy, neglecting the translation of individualized predictions into clinical decision-making guidance [12-14, 26]. Our findings demonstrated that the high-risk group exhibited an approximate 20% incidence of spirometry-defined AO by the

Pre-Proof

Copyright *Chronic Obstructive Pulmonary Diseases: Journal of the COPD Foundation* ©2026
Published online November 24, 2026 https://doi.org/10.15326/jcopdf.2026.0850

third year, whereas the low-risk group showed an incidence of 2%-3%. This model discriminated between populations with varying AO development risks, providing a foundation for implementing stratified intervention strategies. Based on the model predictions, it is recommended that high-risk individuals undergo lung examinations (including spirometry) to enable timely detection of AO and facilitate early intervention, while low-risk individuals may undergo less spirometry screening. Furthermore, we developed an online application platform for this risk stratification model, which processes user data to deliver risk assessment outcomes, thereby assisting clinicians in decision making and facilitating the clinical implementation of artificial intelligence research. This computational process is currently limited to the research setting. To enhance its practical feasibility, future work will focus on developing an automated application that can compute the radscore directly from user-uploaded CT images and subsequently generate the corresponding risk stratification for airflow obstruction development.

There was no statistical difference in AUCs between the combined, clinical, and radiomic models in the testing dataset. In the two datasets, the combined model exhibited lower Brier scores compared with the radiomic and clinical models, suggesting a trend toward better calibration. While the combined model had lower sensitivity than the clinical model, it demonstrated higher specificity. The clinical model achieved a sensitivity approaching 90%, which may be sufficient for case detection. However, its specificity of approximately 50% may classify some individuals without airflow obstruction development as high risk, potentially leading to over intervention. The combined model exhibited higher F1 scores than the clinical model. This suggests a trend toward slightly better overall performance of the combined model. The combined model is not limited to individualized prediction but further performs risk stratification based on individual predicted probabilities. The risk stratification of the combined

Pre-Proof

Copyright *Chronic Obstructive Pulmonary Diseases: Journal of the COPD Foundation* ©2026
Published online November 24, 2026 https://doi.org/10.15326/jcopdf.2026.0850

model showed slightly better discriminative ability for the rate of lung function decline than the radiomic and clinical models, providing a basis for guiding intervention and management across different risk groups.

The combined model exhibited slightly better predictive performance for stratifying the risk of spirometry-defined AO development compared with the radiomic or clinical models. These results align with previous studies indicating that incorporating CT radiomics features enhances predictive capability [12-13]. Notably, higher radscore correlated with increased the risk of AO development. The selected radiomics features in our study included first order, gray level cooccurrence matrix (GLCM), and gray level size zone matrix (GLSZM) features. First order features quantify voxel intensity distribution, while GLCM and GLSZM features characterize spatial relationships between pixels, reflecting subtle structural lung alterations that are imperceptible on visual assessment [27]. These radiomics features provide additional early pathological information on COPD-related lung changes, complementing baseline clinical data to improve the predictive accuracy for disease progression. The combined model achieved an AUC of 0.807 (95% CI 0.715–0.900), lower than the AUC of 0.877 (95% CI 0.766–0.988) reported previously [26]. The previously reported model incorporated spirometry and quantitative CT parameters alongside demographic and radiomics features, which may explain its enhanced performance. However, given the low utilization of spirometry in primary healthcare settings, our model intentionally incorporated only clinical variables and inspiratory CT to reduce implementation barriers and minimize reliance on spirometry in clinical practice [28].

In the testing dataset of the combined model, the high-risk group demonstrated a higher trend toward spirometry-defined AO development after adjusting for covariates than the low-risk

Pre-Proof

Copyright *Chronic Obstructive Pulmonary Diseases: Journal of the COPD Foundation* ©2026
Published online November 24, 2026 https://doi.org/10.15326/jcopdf.2026.0850

group, though without reaching statistical significance. This may be attributed to the limited sample size of the testing dataset and insufficient follow-up duration, as some high-risk individuals might have already developed accelerated lung function decline without meeting the diagnostic criterion of postbronchodilator $FEV_1/FVC < 0.70$ for airflow obstruction. The high-risk group showed faster annual declines in prebronchodilator FEV_1, postbronchodilator FEV_1, and postbronchodilator FEV_1/FVC than the low-risk group. Consistent with previous findings, the radscore was negatively correlated with lung function, confirming the established relationship between CT radiomics features and spirometry parameters [14,29]. Pre-COPD structural alterations in lung architecture may drive lung function decline, while radiomics features capturing heterogeneous parenchymal abnormalities exhibit predictive capacity for subsequent lung function deterioration.

The combined model was constructed by combining CT radscore with clinical variables. The radscore was calculated from radiomics features extracted from CT images, which were generated by automated quantitative system without visual assessment of the images. Emphysema is one of the pathological features of COPD [1]. Visual imaging assessment can detect significant emphysema in the lung. The presence of emphysema on CT warrants consideration of COPD, the probability of AO development and the corresponding risk stratification can be predicted by the combined model. However, visual imaging assessment is inherently subjective and insensitive to mild emphysema or other subtle lesions, whereas CT radiomics can capture pathological changes that are invisible to the naked eye [11]. Therefore, the combined model and radiology visual interpretation are complementary: the model provides individual-level probabilities of AO development and risk stratification, thereby guiding further intervention and management.

Pre-Proof

Copyright *Chronic Obstructive Pulmonary Diseases: Journal of the COPD Foundation* ©2026
Published online November 24, 2026 https://doi.org/10.15326/jcopdf.2026.0850

The proportion of baseline airflow obstruction in the ECOPD study was 44.5%. However, according to China's 2018 COPD prevalence survey, the estimated prevalence of airflow obstruction among individuals aged 40–80 years is approximately 15% [15]. This discrepancy is attributable to the ECOPD study design. The ECOPD study planned to recruit approximately 1000 participants with and 1000 without airflow obstruction from the community. To enroll comparable numbers of the two groups, all screened participants with airflow obstruction were invited to participate, whereas one of every four participants without airflow obstruction was invited based on the order of spirometry completion. The higher proportion of airflow obstruction in the ECOPD study relative to the real-world population may affect the generalizability of the model, and further validation in other community cohorts is warranted.

This study has limitations. First, variations in CT scanners may have affected the measurement of radiomics features. The distribution of CT scanners was comparable across different datasets or risk stratification. In this study, the majority of participants underwent CT examination using United-imaging scanner, while a minority used Siemens scanner. To enhance model generalizability, future studies should assess the reproducibility of radiomics features extracted from other widely used CT scanners [30]. Second, the limited sample size and short follow-up duration may have obscured detectable differences in disease progression among the participants, potentially contributing to the lack of statistically significant differences in the AUC values between the models [23]. Future validation with larger sample size and longer follow-up duration is needed. Third, the absence of an external validation cohort limited our ability to evaluate the model's generalizability. Nevertheless, we used a held-out testing dataset (30% of data completely unseen during model construction), demonstrating the model's robustness in independent testing. Fourth, the composition of participants in this study was imbalanced, with

Pre-Proof

Copyright *Chronic Obstructive Pulmonary Diseases: Journal of the COPD Foundation* ©2026
Published online November 24, 2026 https://doi.org/10.15326/jcopdf.2026.0850

78.4% of participants having baseline postbronchodilator FEV_1/FVC ratio between 0.70 and 0.75. The model's predictive performance may be confounded by measurement variability near the FEV_1/FVC threshold. Future validation with a more balanced participant composition is warranted. Fifth, using univariate screening for clinical variable selection may lead to model instability. Based on previous studies, our study selected clinical variables most closely associated with COPD development, which may have resulted in the omission of other potentially valuable clinical variables, potentially causing selection bias in model development. Finally, using complete case analysis without imputation leads to reduction in the sample size and statistical power, and may result in the loss of valuable information regarding the relationship between predictors and outcomes.

Conclusions

In conclusion, the spirometry-defined AO development risk prediction model combining CT radiomics features and clinical variables showed potential predictive performance, which may facilitate precise intervention in distinct risk groups. Future research should focus on prospective validation to assess early intervention outcomes when using this risk stratification approach and explore its value in guiding personalized management.

Pre-Proof

Copyright *Chronic Obstructive Pulmonary Diseases: Journal of the COPD Foundation* ©2026
Published online November 24, 2026 https://doi.org/10.15326/jcopdf.2026.0850

Authors' contributions

Guarantors of integrity of entire study, S.H., F.W., K.Z., Z.D., P.R., Y.Z.; study concepts/study design or data acquisition or data analysis/interpretation, all authors; manuscript drafting or manuscript revision for important intellectual content, S.H., F.W., K.Z., Z.D., P.R., Y.Z.; approval of final version of submitted manuscript, all authors; agrees to ensure any questions related to the work are appropriately resolved, all authors; literature research, S.H., F.W.; clinical studies, all authors; experimental studies, S.H., F.W.; statistical analysis, S.H., F.W.; and manuscript editing, all authors. All authors revised the manuscript and approved the final version before submission.

Artificial intelligence involvement

None of the material has been partially or totally produced with the help of any artificial intelligence software or tool.

Acknowledgements

We thank the participants and their families who participated in the ECOPD cohort study. We thank Emily Woodhouse, PhD, from Liwen Bianji (Edanz) (www.liwenbianji.cn) for editing the English text of a draft of this manuscript.

Declarations

Ethics approval and consent to participate: This study was approved by the Ethics Committee of the First Affiliated Hospital of Guangzhou Medical University (No. 2018-53). All participants provided written informed consent.

Consent for publication

No individual participant data is reported that would require consent to publish from the

Pre-Proof

Copyright *Chronic Obstructive Pulmonary Diseases: Journal of the COPD Foundation* ©2026
Published online November 24, 2026 https://doi.org/10.15326/jcopdf.2026.0850

participant.

Availability of data and materials

Data and materials generated or analyzed during the study are available from the corresponding author by request.

Competing interests

Y.C., P.W., and Q.P. are employees of Hangzhou Smart Intelligent Co., Ltd. No other disclosures were reported.

Pre-Proof

Copyright *Chronic Obstructive Pulmonary Diseases: Journal of the COPD Foundation* ©2026
Published online November 24, 2026 https://doi.org/10.15326/jcopdf.2026.0850

References

1. Global Initiative for Chronic Obstructive Lung Disease (GOLD). Global Strategy for the Diagnosis, Management, and Prevention of Chronic Obstructive Lung Disease: 2025 report [Accessed on July 1, 2025]. Available at: https://goldcopd.org/2025-gold-report/
2. De Oca MM, Perez-Padilla R, Celli B, Aaron SD, Wehrmeister FC, Amaral AFS, et al. The global burden of COPD: epidemiology and effect of prevention strategies. Lancet Respir Med 2025;13(8):709-724
3. Bhatt SP, Rabe KF, Hanania NA, Vogelmeier CF, Cole J, Bafadhel M, et al. Dupilumab for COPD with Type 2 Inflammation Indicated by Eosinophil Counts. N Engl J Med 2023;389(3):205-214
4. Rabe KF, Martinez FJ, Ferguson GT, Wang C, Singh D, Wedzicha JA, et al. Triple Inhaled Therapy at Two Glucocorticoid Doses in Moderate-to-Very-Severe COPD. N Engl J Med 2020;383(1):35-48
5. Stolz D, Mkorombindo T, Schumann DM, Agusti A, Ash SY, Bafadhel M, et al. Towards the elimination of chronic obstructive pulmonary disease: a Lancet Commission. Lancet 2022;400(10356):921-972
6. Martinez FJ, Han MK, Allinson JP, Barr RG, Boucher RC, Calverley PMA, et al. At the Root: Defining and Halting Progression of Early Chronic Obstructive Pulmonary Disease. Am J Respir Crit Care Med 2018;197(12):1540-1551
7. Divo MJ, Liu C, Polverino F, Castaldi PJ, Celli BR, Tesfaigzi Y. From pre-COPD to COPD: a Simple, Low cost and easy to IMplement (SLIM) risk calculator. Eur Respir J 2023;62(3)
8. Tan DJ, Lodge CJ, Walters EH, Bui DS, Pham J, Lowe AJ, et al. Can We Use Lung Function Thresholds and Respiratory Symptoms to Identify Pre-Chronic Obstructive Pulmonary

Pre-Proof

Copyright *Chronic Obstructive Pulmonary Diseases: Journal of the COPD Foundation* ©2026
Published online November 24, 2026 https://doi.org/10.15326/jcopdf.2026.0850

Disease? A Prospective, Population-based Cohort Study. Am J Respir Crit Care Med 2024;209(12):1431-1440

9. Verleden SE, Hendriks JMH, Snoeckx A, Mai C, Mentens Y, Callebaut W, et al. Small Airway Disease in Pre-Chronic Obstructive Pulmonary Disease with Emphysema: A Cross-Sectional Study. Am J Respir Crit Care Med 2024;209(6):683-692
10. Lambin P, Rios-Velazquez E, Leijenaar R, Carvalho S, van Stiphout RG, Granton P, et al. Radiomics: extracting more information from medical images using advanced feature analysis. Eur J Cancer 2012;48(4):441-446
11. Lambin P, Leijenaar RTH, Deist TM, Peerlings J, de Jong EEC, van Timmeren J, et al. Radiomics: the bridge between medical imaging and personalized medicine. Nat Rev Clin Oncol 2017;14(12):749-762
12. Amudala Puchakayala PR, Sthanam VL, Nakhmani A, Chaudhary MFA, Kizhakke Puliyakote A, Reinhardt JM, et al. Radiomics for Improved Detection of Chronic Obstructive Pulmonary Disease in Low-Dose and Standard-Dose Chest CT Scans. Radiology 2023;307(5):e222998
13. Zhou TH, Zhou XX, Ni J, Ma YQ, Xu FY, Fan B, et al. CT whole lung radiomic nomogram: a potential biomarker for lung function evaluation and identification of COPD. Mil Med Res 2024;11(1):14
14. Makimoto K, Hogg JC, Bourbeau J, Tan WC, Kirby M. Enhancing COPD classification using combined quantitative computed tomography and texture-based radiomics: a CanCOLD cohort study. ERJ Open Res 2024;10(4)
15. Wang C, Xu J, Yang L, et al. Prevalence and risk factors of chronic obstructive pulmonary disease in China (the China Pulmonary Health [CPH] study): a national cross-sectional

Pre-Proof

Copyright *Chronic Obstructive Pulmonary Diseases: Journal of the COPD Foundation* ©2026
Published online November 24, 2026 https://doi.org/10.15326/jcopdf.2026.0850

study. Lancet. 2018;391(10131):1706-1717

16. Wu F, Zhou Y, Peng J, Deng Z, Wen X, Wang Z, et al. Rationale and design of the Early Chronic Obstructive Pulmonary Disease (ECOPD) study in Guangdong, China: a prospective observational cohort study. J Thorac Dis 2021;13(12):6924-6935
17. Zhong N, Wang C, Yao W, Chen P, Kang J, Huang S, et al. Prevalence of chronic obstructive pulmonary disease in China: a large, population-based survey. Am J Respir Crit Care Med 2007;176(8):753-760
18. Miller MR, Crapo R, Hankinson J, Brusasco V, Burgos F, Casaburi R, et al. General considerations for lung function testing. Eur Respir J 2005;26(1):153-161
19. Miller MR, Hankinson J, Brusasco V, Burgos F, Casaburi R, Coates A, et al. Standardisation of spirometry. Eur Respir J 2005;26(2):319-338
20. Zwanenburg A, Vallières M, Abdalah MA, Aerts H, Andrearczyk V, Apte A, et al. The Image Biomarker Standardization Initiative: Standardized Quantitative Radiomics for High-Throughput Image-based Phenotyping. Radiology 2020;295(2):328-338
21. Collins GS, Reitsma JB, Altman DG, Moons KG. Transparent reporting of a multivariable prediction model for individual prognosis or diagnosis (TRIPOD): the TRIPOD statement. Bmj 2015;350:g7594
22. Westfall P. Simultaneous small-sample multivariate Bernoulli confidence intervals. Biometrics 1985;41(4):1001-1013
23. DeLong ER, DeLong DM, Clarke-Pearson DL. Comparing the areas under two or more correlated receiver operating characteristic curves: a nonparametric approach. Biometrics 1988;44(3):837-845
24. Qu L, Zhu J, Mei X, Yi Z, Luo N, Yuan S, et al. Evaluating axillary lymph node metastasis

Pre-Proof

Copyright *Chronic Obstructive Pulmonary Diseases: Journal of the COPD Foundation* ©2026
Published online November 24, 2026 https://doi.org/10.15326/jcopdf.2026.0850

risks in breast cancer patients via Semi-ALNP: a multicenter study. EClinicalMedicine 2025;85:103311

25. Laird NM, Ware JH. Random-effects models for longitudinal data. Biometrics 1982;38(4):963-974
26. Makimoto K, Hogg JC, Bourbeau J, Tan WC, Kirby M. CT Imaging With Machine Learning for Predicting Progression to COPD in Individuals at Risk. Chest 2023;164(5):1139-1149
27. Mayerhoefer ME, Materka A, Langs G, Häggström I, Szczypiński P, Gibbs P, et al. Introduction to Radiomics. J Nucl Med 2020;61(4):488-495
28. Dehondt V, Vauterin D, Derom E, Lahousse L. Association of Timely Spirometry With Lower All-Cause Mortality: A Nationwide Obstructive Cohort Study. Chest 2025; 168(3):602-612
29. Koo MC, Au R, Hague CJ, Leipsic JA, Tan WC, Hogg JC, et al. Expiration CT Gas Trapping Measures with Texture-Based Radiomics Improves Association with Lung Function and Lung Function Decline in COPD. Acad Radiol 2025;32(6):3711-3721
30. Yasaka K, Akai H, Mackin D, Court L, Moros E, Ohtomo K, et al. Precision of quantitative computed tomography texture analysis using image filtering: A phantom study for scanner variability. Medicine (Baltimore) 2017;96(21):e6993

Pre-Proof

Copyright *Chronic Obstructive Pulmonary Diseases: Journal of the COPD Foundation* ©2026
Published online November 24, 2026 https://doi.org/10.15326/jcopdf.2026.0850

Table 1. Baseline characteristics.

Characteristic	Training dataset (n=656)			Testing dataset (n=281)		
	No progression to AO (n=587)	Progression to AO (n=69)	P Value	No progression to AO (n=254)	Progression to AO (n=27)	P Value
Age — year	58.0±7.7	63.0±7.5	**<0.001**	58.0±7.1	63.0±7.0	**<0.001**
Male sex — no. (%)	326 (55.5)	62 (89.9)	**<0.001**	144 (56.7)	24 (88.9)	**0.001**
Body mass index — kg/m^2	23.6±3.1	22.5±3.0	**0.007**	23.5±3.2	21.6±2.9	**0.004**
Smoking status — no. (%)			**<0.001**			**0.002**
Never smoked	337 (57.4)	17 (24.6)		141 (55.5)	6 (22.2)	
Former smoked	73 (12.4)	17 (24.6)		33 (13.0)	4 (14.8)	
Current smoked	177 (30.2)	35 (50.7)		80 (31.5)	17 (63.0)	
Smoking index — pack-year	17.6±29.3	31.3±28.0	**<0.001**	18.5±28.7	28.6±25.7	0.080
Biomass exposure — no. (%)	204 (34.8)	25 (36.2)	0.807	86 (33.9)	6 (22.2)	0.221
Occupational history of dusts/gases/fumes — no. (%)	104 (17.7)	13 (18.8)	0.818	35 (13.8)	7 (25.9)	0.149
Family history of respiratory diseases — no. (%)	52 (8.9)	12 (17.4)	**0.024**	24 (9.4)	3 (11.1)	0.732
Respiratory symptoms — no. (%)						
Chronic cough	94 (16.0)	12 (17.4)	0.769	44 (17.3)	6 (22.2)	0.595
Chronic sputum production	151 (25.7)	20 (29.0)	0.559	59 (23.2)	6 (22.2)	0.906
Dyspnea	111 (18.9)	15 (21.7)	0.572	62 (24.4)	6 (22.2)	0.801
Wheeze	28 (4.8)	3 (4.3)	1.000	22 (8.7)	3 (11.1)	0.719
mMRC score	0.22±0.49	0.25±0.50	0.653	0.29±0.55	0.22±0.42	0.550
CAT score	3.1±4.2	3.5±4.9	0.489	3.1±3.7	2.7±3.6	0.593
Spirometry						
Prebronchodilator FEV_1 — L	2.33±0.55	2.34±0.55	0.951	2.36±0.58	2.30±0.50	0.617
Postbronchodilator FEV_1 — L	2.41±0.54	2.44±0.56	0.699	2.41±0.57	2.41±0.52	0.964
Postbronchodilator FEV_1/FVC — %	79.7±5.5	73.6±3.4	**<0.001**	79.5±5.3	73.3±3.0	**<0.001**
Computed tomography						
Radscore	-2.56 (-3.11, -1.97)	-1.68 (-2.20, -1.02)	**<0.001**	-2.44 (-3.00, -1.90)	-1.56 (-2.12, -1.34)	**<0.001**

Data are presented as mean ± standard deviation, median (interquartile range), or n (%).

Abbreviation: AO, airflow obstruction; CAT, chronic obstructive pulmonary disease assessment test; FEV_1, forced expiratory volume in 1 second; FVC, forced vital capacity; mMRC, the modified Medical Research Council.

Pre-Proof

Copyright *Chronic Obstructive Pulmonary Diseases: Journal of the COPD Foundation* ©2026
Published online November 24, 2026 https://doi.org/10.15326/jcopdf.2026.0850

Table 2. Performance of models for predicting spirometry-defined airflow obstruction development in the training and testing datasets.

Model	AUC (95%CI)	Accuracy (%)	Sensitivity (%)	Specificity (%)	PPV (%)	NPV (%)	F1 score
Clinical model							
Training dataset	0.761 (0.707 to 0.815)	57.3	89.9	53.4	18.5	97.8	0.307
Testing dataset	0.777 (0.688 to 0.865)	56.2	88.9	52.8	16.7	97.8	0.281
Radiomic model							
Training dataset	0.785 (0.731 to 0.839)	73.5	71.0	73.8	24.1	95.6	0.360
Testing dataset	0.774 (0.681 to 0.866)	71.2	74.1	70.9	21.3	96.3	0.331
Combined model							
Training dataset	0.807 (0.757 to 0.856)	68.1	85.5	66.0	22.9	97.5	0.361
Testing dataset	0.807 (0.715 to 0.900)	63.4	81.5	61.4	18.3	96.9	0.299

Abbreviation: AO, airflow obstruction; AUC, area under the receiver operating characteristic curve; CI, confidence interval; PPV, positive predictive value, NPV, negative predictive value.

Pre-Proof

Copyright *Chronic Obstructive Pulmonary Diseases: Journal of the COPD Foundation* ©2026
Published online November 24, 2026 https://doi.org/10.15326/jcopdf.2026.0850

Figure Legends

Figure 1. The pipeline of spirometry-defined airflow obstruction development risk-stratification.

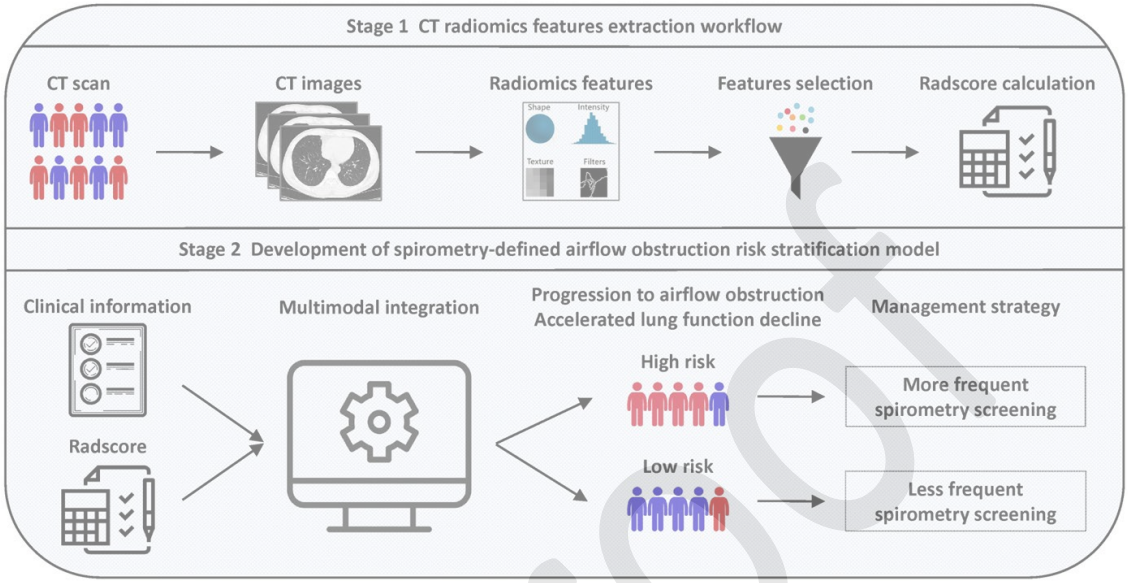

Abbreviations: AO, airflow obstruction; CT, computed tomography.

Figure 2. Features selection, machine learning algorithms, and performance evaluation of unimodal and multimodal models in predicting spirometry-defined airflow obstruction development.

Pre-Proof

Copyright *Chronic Obstructive Pulmonary Diseases: Journal of the COPD Foundation* ©2026
Published online November 23, 2026 https://doi.org/10.15326/jcopdf.2026.0850

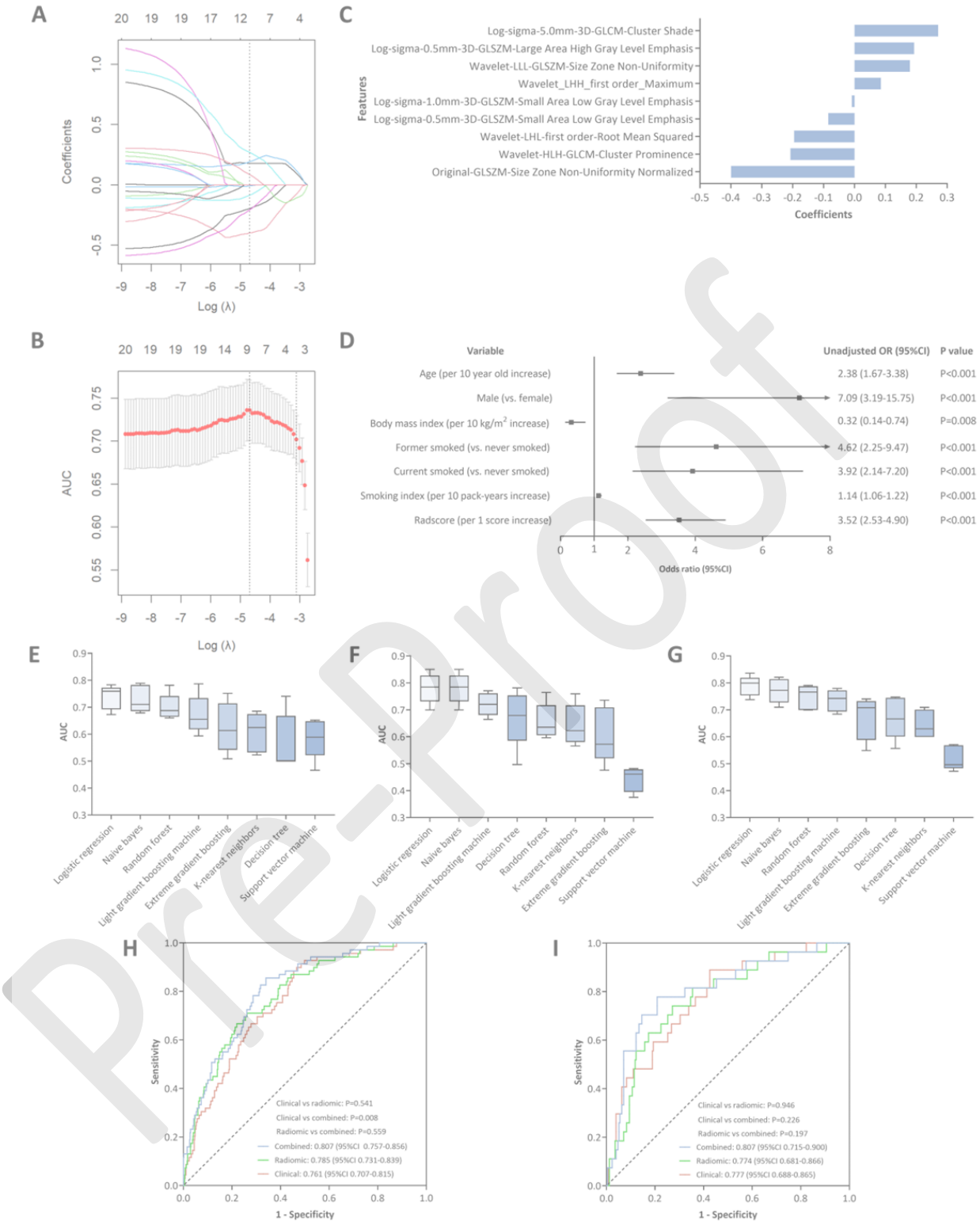

(A) LASSO coefficient profiles of the 20 radiomic features. The optimal λ value was identified via 10-fold cross-validation by plotting a vertical line at the log (λ) position. The optimal λ value (0.00919) resulted in the retention of 9 radiomic features.

(B) Selection of the optimal tuning parameter in the LASSO model based on minimum

Pre-Proof

Copyright *Chronic Obstructive Pulmonary Diseases: Journal of the COPD Foundation* ©2026
Published online November 23, 2026 https://doi.org/10.15326/jcopdf.2026.0850

criteria. The two vertical lines were plotting based on minimum criteria and 1-s.e. criteria.

(C) Histogram of the selected 9 radiomic features.

(D) Univariable regression analysis of factors potentially affecting AO development in the training dataset.

(E) Selection of the machine learning algorithms in clinical model.

(F) Selection of the machine learning algorithms in radiomic model.

(G) Selection of the machine learning algorithms in combined model.

(H) ROC curves of three models in predicting AO development in the training dataset.

(I) ROC curves of three models in predicting AO development in the testing dataset.

Abbreviations: AO, airflow obstruction; AUC, area under the receiver operating characteristic curve; CI, confidence interval; LASSO, least absolute shrinkage and selection operator; ROC, receiver operating characteristic; OR, odds ratio.

Figure 3. Chronic obstructive pulmonary disease development risk stratified by spirometry-defined airflow obstruction risk stratification in the combined model.

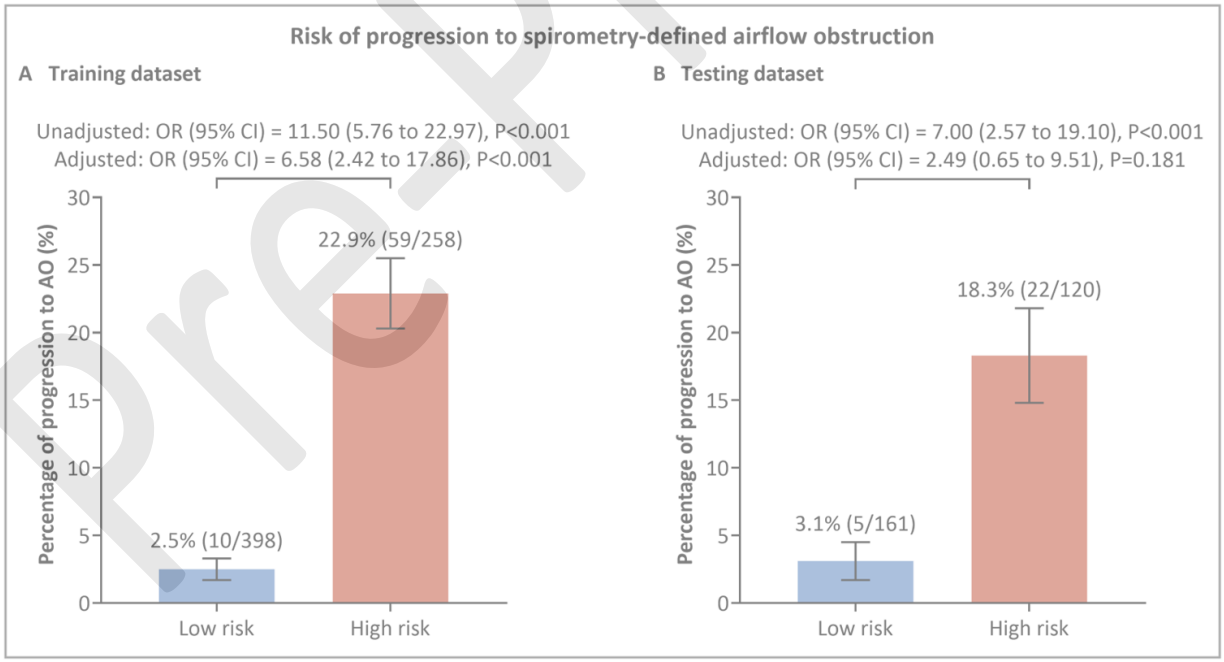

Data are presented as n (%).

Abbreviation: AO, airflow obstruction; CI, confidence interval; OR, odds ratio.

Figure 4. Annual decline in lung function stratified by spirometry-defined airflow obstruction risk stratification in the combined model.

Pre-Proof

Copyright *Chronic Obstructive Pulmonary Diseases: Journal of the COPD Foundation* ©2026
Published online November 23, 2026 https://doi.org/10.15326/jcopdf.2026.0850

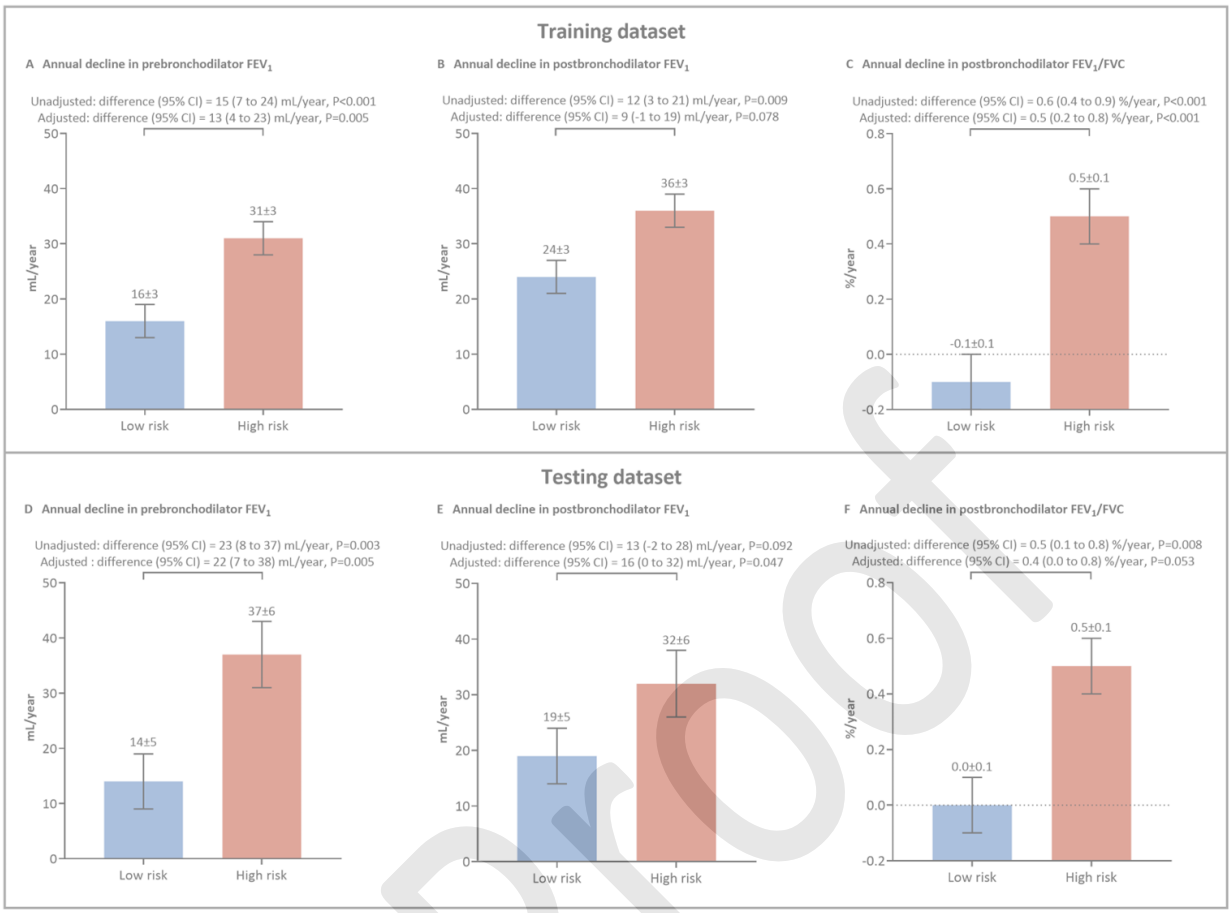

Data are presented as mean ± standard error.

Abbreviation: CI, confidence interval; FEV_1, forced expiratory volume in 1 second; FVC, forced vital capacity.

Figure 5. The calculator for predicting risk stratification of spirometry-defined airflow obstruction development.

Pre-Proof

Copyright *Chronic Obstructive Pulmonary Diseases: Journal of the COPD Foundation* ©2026
Published online November 23, 2026 https://doi.org/10.15326/jcopdf.2026.0850

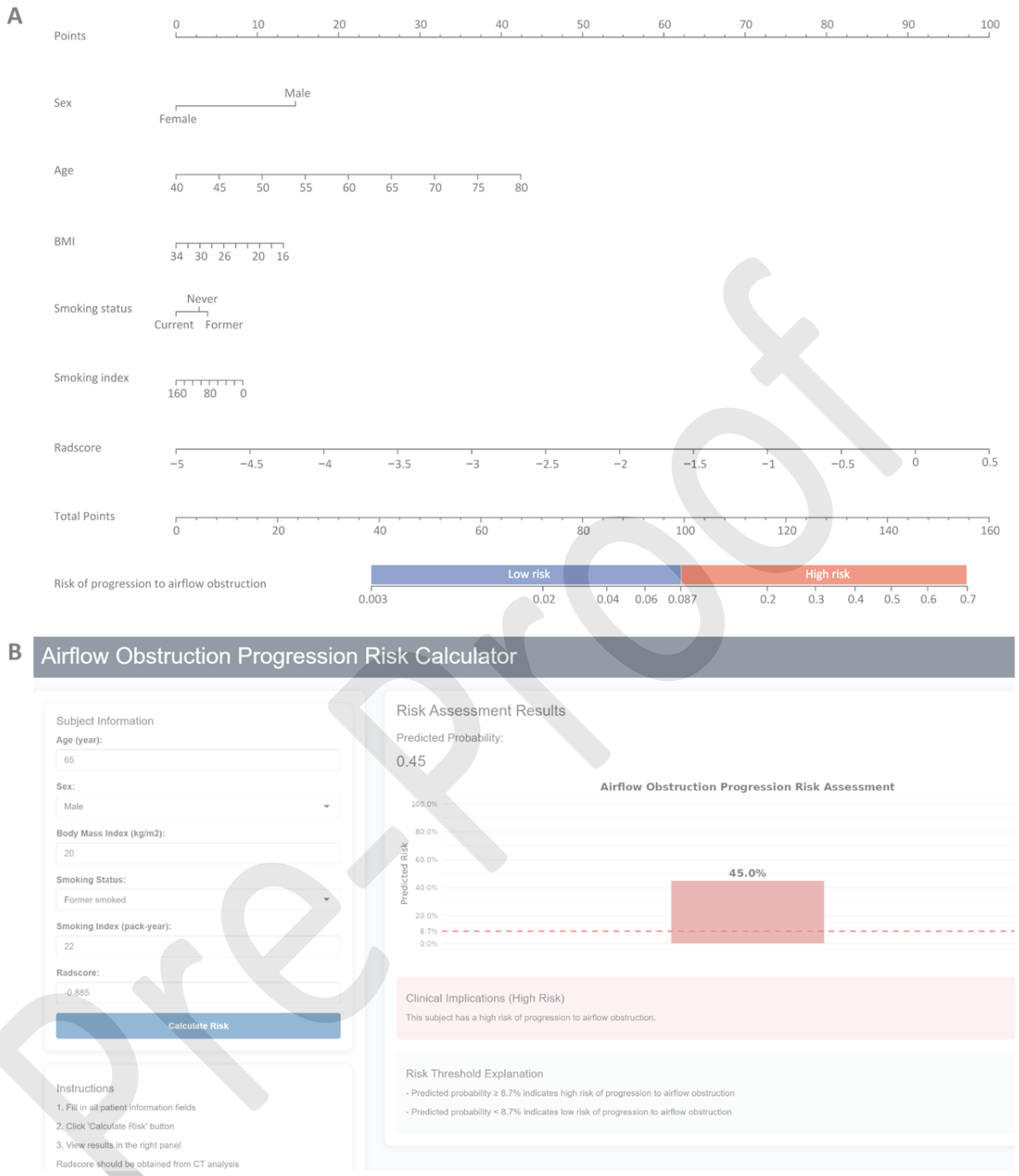

Abbreviation: BMI, body mass index.

Pre-Proof

Copyright *Chronic Obstructive Pulmonary Diseases: Journal of the COPD Foundation* ©2026
Published online November 23, 2026 https://doi.org/10.15326/jcopdf.2026.0850

Methods

Criteria for participant enrollment in the Early Chronic Obstructive Pulmonary Disease study

The inclusion criteria for the Early Chronic Obstructive Pulmonary Disease study were (1) participants aged 40-80 years; (2) completion of standardized respiratory epidemiology questionnaires, chronic respiratory symptoms, pre- and post-bronchodilator spirometry, and chest computed tomography (CT) scans at baseline. The exclusion criteria were (1) respiratory infection or acute respiratory events within 4 weeks prior to screening; (2) history of lung lobectomy; (3) newly diagnosed malignancy undergoing treatment; and (4) lung cancer, active pulmonary tuberculosis, pneumoconiosis, or other serious lung diseases.

Questionnaires

Chronic obstructive pulmonary disease (COPD)-related risk factors and chronic respiratory symptoms were collected. COPD-related risk factors included smoking status, smoking index, biomass exposure, occupational exposure, and family history of respiratory diseases. Chronic respiratory symptoms, including dyspnea, chronic cough, chronic sputum expectoration, and wheezing, were self-reported by the participants. The COPD Assessment Test was used to evaluate respiratory-related quality of life, while the Medical Research Council scale was used to assess dyspnea severity [1-2].

Spirometry

For each participant, at least three acceptable measurement curves with two repeatable curves (maximum and submaximum forced vital capacity and forced expiratory volume in 1 second within 150mL or 5%, respectively) were obtained.

Pre-Proof

Copyright *Chronic Obstructive Pulmonary Diseases: Journal of the COPD Foundation* ©2026
Published online November 23, 2026 https://doi.org/10.15326/jcopdf.2026.0850

Following prebronchodilator spirometry, postbronchodilator spirometry testing was conducted 20 min after the administration of 400 μg salbutamol. The lower limit of normal (LLN) of lung function were determined using the Global Lung Initiative race-neutral prediction formula [3].

CT image acquisition, segmentation, and preprocessing

All participants underwent inspiratory chest CT in the supine position from the lung apex to the base. The CT scanning parameters were as follows: 120 kVp, 200 mA, 0.5 second exposure, 1.1 pitch, and 0.75-mm slice thickness. The CT images were reconstructed using a 512 × 512-pixel matrix [4-5]. The CT scan protocol and the distribution of CT scanners are shown in the **Supplementary Table S1** and **Supplementary Table S2**, respectively. The inspiratory CT scans were acquired at the end of deep inspiration. The left and right lungs were segmented using AVIEW software (1.1.42.2001-win, Coreline Soft Co. Ltd.) and subsequently merged into a combined region of interest. The CT images were preprocessed following the Image Biomarker Standardization Initiative guidelines [6]. First, the images were resampled to a voxel size of 1 × 1 × 1 mm^3 using B-spline interpolation. Second, gray-level intensities were discretized into a finite number of bins, a bin width of 10 was applied [7]. Third, the voxel array shift was set to 1024, and the segmentation label with value 1 was used as the region of interest.

Radiomics features extraction and selection

A total of 1239 CT radiomics features were extracted (**Supplementary Table S3**). The original features included 19 first order, 24 gray level cooccurrence matrix (GLCM), 16 gray level run length matrix (GLRLM), 16 gray level size zone matrix (GLSZM), 14 gray level dependence matrix (GLDM), 5 neighborhood gray tone difference matrix

Pre-Proof

Copyright *Chronic Obstructive Pulmonary Diseases: Journal of the COPD Foundation* ©2026
Published online November 23, 2026 https://doi.org/10.15326/jcopdf.2026.0850

(NGTDM) and 17 shape-based features. Moreover, 376 wavelet features were derived using configured wavelet filters based on the first order and texture features, while 752 Laplacian of Gaussian (LoG) features were generated by LoG filtering with kernel sizes of 0.5, 1.0, 3.0, and 5.0 mm. The key parameters for CT radiomic feature extraction using PyRadiomics were as follows. The image types were set to include the original image, LoG filtered images (with sigma values of 0.5, 1.0, 3.0, and 5.0), and wavelet decompositions (yielding eight sub-bands: LHH, HLL, HLH, HHL, LLH, HHH, LLL, and LHL). Feature classes were set to first order, GLCM, GLRLM, GLSZM, GLDM, NGTDM and shape-based features.

The radiomics features in the training dataset were standardized using Z-score normalization to eliminate scale differences among the features. The normalization parameters derived from the training dataset were subsequently applied to the testing dataset to ensure preprocessing consistency. The Z-score normalization formula and normalization parameters for the selected features are provided in the **Supplementary Calculation formula** and **Supplementary Table S4**, respectively. To avoid model overfitting, dimensionality reduction was performed through the following steps: removal of features with Spearman's correlation coefficients greater than 0.90, application of the minimum redundancy maximum relevance algorithm to eliminate redundant features, and selection of an optimal feature subset by the Least Absolute Shrinkage and Selection Operator regression with 10-fold cross-validation, choosing features that minimized the binomial deviance [8-9].

Model construction

We evaluated multiple classical and commonly used machine learning algorithms, including logistic regression, naive bayes, random forest, k-nearest neighbors,

Pre-Proof

Copyright *Chronic Obstructive Pulmonary Diseases: Journal of the COPD Foundation* ©2026
Published online November 23, 2026 https://doi.org/10.15326/jcopdf.2026.0850

decision tree, support vector machine, extreme gradient boosting, and light gradient boosting machine in the training dataset. Each model was trained using default parameters, followed by performance evaluation. To select the optimal model hyperparameters, a combination of 5-fold cross-validation and grid search technique was applied. We used a benchmarking tool to evaluate the performance of the different machine learning algorithms. The optimal machine learning algorithm, determined by the highest mean area under the receiver operating characteristic curve (AUC), was used for model construction. In cases where the AUC values were equal, the simpler and more interpretable algorithms were prioritized to ensure methodological transparency. The mean AUC values of the machine learning algorithms in the training dataset are shown in the **Supplementary Table S7**.

Statistical analysis

Random coefficient models with both random intercept and random slope were used to fit the 4 spirometry measures and compare the annual decline in lung function between groups [10-11]. In the final model, lung function at each visit was the dependent variable, different groups were fixed-effect independent variables, baseline lung function of this parameter was the covariate, confounders were fixed-effect confounders, and participants were random intercept. The interaction term between visit and group was included in the model to account for time-varying effects. The annual decline in lung function for each group was expressed as regression coefficients. The selection of the appropriate covariance structure type was achieved by considering the biological characteristics of the lung function decline and selecting the smallest Akaike information criterion after fitting the model with alternative covariance structures. The final model adopts the variance structure of autoregressive

Pre-Proof

Copyright *Chronic Obstructive Pulmonary Diseases: Journal of the COPD Foundation* ©2026
Published online November 23, 2026 https://doi.org/10.15326/jcopdf.2026.0850

order 1 structure covariance. We used likelihood-based methods to handle missing data for the repeated-measures.

Pre-Proof

Copyright *Chronic Obstructive Pulmonary Diseases: Journal of the COPD Foundation* ©2026
Published online November 23, 2026 https://doi.org/10.15326/jcopdf.2026.0850

References

1. Jones PW, Harding G, Berry P, Wiklund I, Chen WH, Kline Leidy N. Development and first validation of the COPD Assessment Test. Eur Respir J 2009;34(3):648-654
2. Bestall JC, Paul EA, Garrod R, Garnham R, Jones PW, Wedzicha JA. Usefulness of the Medical Research Council (MRC) dyspnoea scale as a measure of disability in patients with chronic obstructive pulmonary disease. Thorax 1999;54(7):581-586
3. Bowerman C, Bhakta NR, Brazzale D, et al. A Race-neutral Approach to the Interpretation of Lung Function Measurements. Am J Respir Crit Care Med. 2023;207(6):768-774
4. Wu F, Zhou Y, Peng J, Deng Z, Wen X, Wang Z, et al. Rationale and design of the Early Chronic Obstructive Pulmonary Disease (ECOPD) study in Guangdong, China: a prospective observational cohort study. J Thorac Dis 2021;13(12):6924-6935
5. Regan EA, Hokanson JE, Murphy JR, Make B, Lynch DA, Beaty TH, et al. Genetic epidemiology of COPD (COPDGene) study design. Copd 2010;7(1):32-43
6. Zwanenburg A, Vallières M, Abdalah MA, Aerts H, Andrearczyk V, Apte A, et al. The Image Biomarker Standardization Initiative: Standardized Quantitative Radiomics for High-Throughput Image-based Phenotyping. Radiology 2020;295(2):328-338
7. Au RC, Tan WC, Bourbeau J, Hogg JC, Kirby M. Impact of image pre-processing methods on computed tomography radiomics features in chronic obstructive pulmonary disease. Phys Med Biol 2021;66(24)
8. Makimoto K, Au R, Moslemi A, Hogg JC, Bourbeau J, Tan WC, et al. Comparison of Feature Selection Methods and Machine Learning Classifiers for Predicting Chronic Obstructive Pulmonary Disease Using Texture-Based CT Lung Radiomic Features. Acad Radiol 2023;30(5):900-910

Pre-Proof

Copyright *Chronic Obstructive Pulmonary Diseases: Journal of the COPD Foundation* ©2026
Published online November 23, 2026 https://doi.org/10.15326/jcopdf.2026.0850

9. De Jay N, Papillon-Cavanagh S, Olsen C, El-Hachem N, Bontempi G, Haibe-Kains B. mRMRe: an R package for parallelized mRMR ensemble feature selection. Bioinformatics 2013;29(18):2365-2368

10. Laird NM, Ware JH. Random-effects models for longitudinal data. Biometrics. 1982;38(4):963-974

11. Vestbo J, Edwards LD, Scanlon PD, et al. Changes in forced expiratory volume in 1 second over time in COPD. N Engl J Med. 2011;365(13):1184-1192

Pre-Proof

Copyright *Chronic Obstructive Pulmonary Diseases: Journal of the COPD Foundation* ©2026
Published online November 23, 2026 https://doi.org/10.15326/jcopdf.2026.0850

The calculation formula for Z-score normalization

$Z=(\chi-\mu)/\sigma$

Note: χ represents the input value, μ represents the mean, and σ represents the standard deviation.

The calculation formula for the radscore

Radscore = 0.271 × log-sigma-5.0mm-3D-GLCM-Cluster Shade + 0.193 × log-sigma-0.5mm-3D-GLSZM-Large Area High Gray Level Emphasis + 0.179 × wavelet-LLL-GLSZM-Size Zone Non-Uniformity + 0.085 × wavelet-LHH-first order-Maximum + (-0.009) × log-sigma-1.0mm-3D-GLSZM-Small Area Low Gray Level Emphasis + (-0.085) × log-sigma-0.5mm-3D-GLSZM-Small Area Low Gray Level Emphasis + (-0.195) × wavelet-LHL-first order-Root Mean Squared + (-0.208) × wavelet-HLH-GLCM-Cluster Prominence + (-0.399) × original-GLSZM-Size Zone Non-Uniformity Normalized - 2.429

The calculation formula for predicted probability in the combined model

Logit = (-3.240) + 0.061 × age + (-0.041) × BMI + 1.032 × radscore + 0.828 × I (sex="Male") + (-0.003) × smoking index + 0.063 × I (smoking status="Former smoked") + (-0.155) × I (smoking status="Current smoked")

P = 1 / (1 + exp(-logit))

Note: P represents the probability of airflow obstruction development.

I (·) is the indicator function, which takes the value 1 if the condition holds and 0 otherwise.

Pre-Proof

Copyright *Chronic Obstructive Pulmonary Diseases: Journal of the COPD Foundation* ©2026
Published online November 23, 2026 https://doi.org/10.15326/jcopdf.2026.0850

Table S1. CT scanning parameters.

Scanner Manufacturer	Siemens	United-imaging
Scan model	Definition (AS Plus), 128-slices	uCT 760, 128-slices
Scan type	Spiral	Spiral
Scan FOV	Lungs	Lungs
Rotation time, s	0.5	0.5
Pitch	1.1	1.1
kVp	120	120
Inspiratory mAs	Effective mAs 200	Effective mAs 200
Expiratory mAs	Effective mAs 50	Effective mAs 50
Dose modulation	Care dose off	Care dose off
Algorithm 1	B35f	B_SOFT_B
Algorithm 2	B46f	B_SHARP_C
Matrix	512×512	512×512
Additional image filters	No selection	No selection
Thickness, mm	0.75	0.75
Interval, mm	0.5	0.5

Abbreviation: FOV, field of view.

Pre-Proof

Copyright *Chronic Obstructive Pulmonary Diseases: Journal of the COPD Foundation* ©2026
Published online November 23, 2026 https://doi.org/10.15326/jcopdf.2026.0850

Table S2. CT scanner distribution.

Scanner Manufacturer	Siemens	United-imaging
Dataset — no. (%)		
Training dataset	89 (13.6)	567 (86.4)
Testing dataset	40 (14.2)	241 (85.8)
Training dataset — no. (%)		
Low risk of combined model	38 (9.5)	360 (90.5)
High risk of combined model	51 (19.8)	207 (80.2)
Testing dataset — no. (%)		
Low risk of combined model	18 (11.2)	143 (88.8)
High risk of combined model	22 (18.3)	98 (81.7)

Data are presented as n (%).

Pre-Proof

Copyright *Chronic Obstructive Pulmonary Diseases: Journal of the COPD Foundation* ©2026
Published online November 23, 2026 https://doi.org/10.15326/jcopdf.2026.0850

Table S3. Summary of CT radiomics features extracted via PyRadiomics.

Features category	Number of Features
Original shape features	
Compactness1	1
Compactness2	1
Elongation	1
Flatness	1
Maximum 2D Diameter Column	1
Maximum 2D Diameter Row	1
Maximum 2D Diameter Slice	1
Maximum 3D Diameter	1
Major Axis Length	1
Minor Axis Length	1
Least Axis Length	1
Sphericity	1
Surface Area	1
Surface Volume Ratio	1
Mesh Volume	1
Voxel Volume	1
Spherical Disproportion	1
Original first order features	
10 Percentile	1
90 Percentile	1
Energy	1
Total Energy	1
Entropy	1
Interquartile Range	1
Kurtosis	1
Maximum	1
Mean	1
Mean Absolute Deviation	1
Median	1
Minimum	1
Range	1
Root Mean Squared	1
Skewness	1
Standard Deviation	1
Uniformity	1
Variance	1
Robust Mean Absolute Deviation	1
Original GLCM texture features	
Informational Measure of Correlation 1	1
Informational Measure of Correlation 2	1
Inverse Variance	1

Pre-Proof

Copyright *Chronic Obstructive Pulmonary Diseases: Journal of the COPD Foundation* ©2026
Published online November 23, 2026 https://doi.org/10.15326/jcopdf.2026.0850

Joint Average	1
Joint Energy	1
Joint Entropy	1
Maximal Correlation Coefficient	1
Maximum Probability	1
Sum Average	1
Sum Entropy	1
Sum Squares	1
Autocorrelation	1
Cluster Prominence	1
Cluster Shade	1
Cluster Tendency	1
Contrast	1
Correlation	1
Difference Average	1
Difference Entropy	1
Difference Variance	1
Inverse Difference	1
Inverse Difference Moment	1
Inverse Difference Moment Normalized	1
Inverse Difference Normalized	1
Original GLDM texture features	
Dependence Entropy	1
Dependence Non-Uniformity	1
Dependence Non-Uniformity Normalized	1
Dependence Variance	1
Gray Level Non-Uniformity	1
Gray Level Variance	1
High Gray Level Emphasis	1
Large Dependence Emphasis	1
Large Dependence High Gray Level Emphasis	1
Large Dependence Low Gray Level Emphasis	1
Low Gray Level Emphasis	1
Small Dependence Emphasis	1
Small Dependence High Gray Level Emphasis	1
Small Dependence Low Gray Level Emphasis	1
Original GLRLM texture features	1
Gray Level Non-Uniformity	1
Gray Level Non-Uniformity Normalized	1
Gray Level Variance	1
High Gray Level Run Emphasis	1
Long Run Emphasis	1
Long Run High Gray Level Emphasis	1
Long Run Low Gray Level Emphasis	1

Pre-Proof

Copyright *Chronic Obstructive Pulmonary Diseases: Journal of the COPD Foundation* ©2026
Published online November 23, 2026 https://doi.org/10.15326/jcopdf.2026.0850

Low Gray Level Run Emphasis	1
Run Entropy	1
Run Length Non-Uniformity	1
Run Length Non-Uniformity Normalized	1
Run Percentage	1
Run Variance	1
Short Run Emphasis	1
Short Run High Gray Level Emphasis	1
Short Run Low Gray Level Emphasis	1
Original GLSZM texture features	
Gray Level Non-Uniformity	1
Gray Level Non-Uniformity Normalized	1
Gray Level Variance	1
High Gray Level Zone Emphasis	1
Large Area Emphasis	1
Large Area High Gray Level Emphasis	1
Large Area Low Gray Level Emphasis	1
Low Gray Level Zone Emphasis	1
Size Zone Non-Uniformity	1
Size Zone Non-Uniformity Normalized	1
Small Area Emphasis	1
Small Area High Gray Level Emphasis	1
Small Area Low Gray Level Emphasis	1
Zone Entropy	1
Zone Percentage	1
Zone Variance	1
Original NGTDM texture features	
Busyness	1
Coarseness	1
Complexity	1
Contrast	1
Strength	1
LoG transform features	
Log-sigma-0.5mm-3D-features	94
Log-sigma-1.0mm-3D-features	94
Log-sigma-3.0mm-3D-features	94
Log-sigma-5.0mm-3D-features	94
Wavelet transform features	
Wavelet-LLH features	94
Wavelet-LHL features	94
Wavelet-LHH features	94
Wavelet-HLL features	94
Wavelet-HLH features	94
Wavelet-HHL features	94

Pre-Proof

Copyright *Chronic Obstructive Pulmonary Diseases: Journal of the COPD Foundation* ©2026
Published online November 23, 2026 https://doi.org/10.15326/jcopdf.2026.0850

Wavelet-HHH features	94
Wavelet-LLL features	94

Abbreviation: GLCM, gray level co-occurrence matrix; GLDM, gray level dependence matrix; GLRLM, gray level run length matrix; GLSZM, gray level size zone matrix; LoG, laplacian of gaussian; NGTDM, neighborhood gray tone difference matrix.

Table S4. The normalization parameters for the selected CT radiomics features in the training dataset.

Feature	Mean	Standard deviation
Wavelet-LLL-GLSZM-Size Zone Non-Uniformity	1144939	204048
Original-GLSZM-Size Zone Non-Uniformity Normalized	0.54477745	0.01355974
Log-sigma-0.5mm-3D-GLSZM-Large Area High Gray Level Emphasis	5134707947	5104315650
Log-sigma-0.5mm-3D-GLSZM-Small Area Low Gray Level Emphasis	0.00034416	0.00018078
Wavelet-LHL-first order-Root Mean Squared	1034.26	1.19
Wavelet-LHH-first order-Maximum	477	95
Log-sigma-1.0mm-3D-GLSZM-Small Area Low Gray Level Emphasis	0.00025423	0.00010099
Log-sigma-5.0mm-3D-GLCM-Cluster Shade	4115	972
Wavelet-HLH-GLCM-Cluster Prominence	7548	2283

Abbreviation: GLCM, gray level co-occurrence matrix; GLSZM, gray level size zone matrix.

Pre-Proof

Copyright *Chronic Obstructive Pulmonary Diseases: Journal of the COPD Foundation* ©2026
Published online November 23, 2026 https://doi.org/10.15326/jcopdf.2026.0850

Table S5. Spearman's correlation coefficients of the radscore with postbronchodilator FEV_1/FVC at the third-year follow-up and annualized change in postbronchodilator FEV_1/FVC.

Dataset	Postbronchodilator FEV_1/FVC (%)		Change in postbronchodilator FEV_1/FVC (%/year)	
	Correlation Coefficient	P value	Correlation Coefficient	P value
Whole dataset	-0.50	**<0.001**	0.15	**<0.001**
Training dataset	-0.50	**<0.001**	0.15	**<0.001**
Testing dataset	-0.49	**<0.001**	0.15	**0.014**

Abbreviation: FEV_1, forced expiratory volume in 1 second; FVC, forced vital capacity.

Pre-Proof

Copyright *Chronic Obstructive Pulmonary Diseases: Journal of the COPD Foundation* ©2026
Published online November 23, 2026 https://doi.org/10.15326/jcopdf.2026.0850

Table S6. Association of radscore with spirometry-defined AO development and lung function decline.

Outcome	Parameter	Radscore (per 1 increase)			
		Unadjusted		Adjusted*	
		Effect Estimate (95%CI)	P value	Effect Estimate (95%CI)	P value
AO development, n (%) †	**Percentage**				
Training dataset	69 (10.5)	3.52 (2.53 to 4.90)	**<0.001**	3.15 (2.03 to 4.91)	**<0.001**
Testing dataset	27 (9.6)	3.22 (1.87 to 5.54)	**<0.001**	2.44 (1.13 to 5.27)	**0.023**
Annual decline in lung function	**Annual decline**				
Training dataset					
Prebronchodilator FEV_1, mL/year	22±2	6 (1 to 11)	**0.017**	10 (4 to 15)	**<0.001**
Postbronchodilator FEV_1, mL/year	29±2	3 (-2 to 9)	0.239	8 (2 to 13)	**0.007**
Postbronchodilator FEV_1/FVC, %/year	0.1±0.1	0.0 (-0.1 to 0.2)	0.672	0.2 (0.1 to 0.4)	**0.005**
Testing dataset					
Prebronchodilator FEV_1, mL/year	24±4	9 (0 to 18)	0.052	14 (5 to 23)	**0.003**
Postbronchodilator FEV_1, mL/year	25±4	0 (-9 to 9)	0.962	5 (-5 to 14)	0.334
Postbronchodilator FEV_1/FVC, %/year	0.2±0.1	0.0 (-0.3 to 0.2)	0.857	0.1 (-0.1 to 0.4)	0.225

Data are mean ± standard error or n (%).
Estimates as β coefficient unless otherwise noted.
Abbreviations: AO, airflow obstruction; CI, confidence interval; FEV_1, forced expiratory volume in 1 s; FVC, forced vital capacity; LAA_{-950}, the percentage of the low- attenuation area below −950 Hounsfield units on full- inspiration CT; LAA_{-856}, the percentage of the low-attenuation area below −856 Hounsfield units on full-expiration CT; Pi 10, square root of wall area of a 10-mm lumen perimeter.
* The analysis was adjusted for age, sex, body mass index, smoking status, smoking index, biomass exposure, occupational history of dusts/gases/fumes, family history of respiratory diseases, inspiratory LAA_{-950}, expiratory LAA_{-856}, Pi 10. For the analysis of annual decline in lung function, the analysis was further adjusted for baseline corresponding spirometric values.
† Odds ratio.

Pre-Proof

Copyright *Chronic Obstructive Pulmonary Diseases: Journal of the COPD Foundation* ©2026
Published online November 23, 2026 https://doi.org/10.15326/jcopdf.2026.0850

Table S7. Performance of machine learning algorithms in the training dataset.

Machine learning algorithm	Clinical model	Radiomic model	Combined model
	AUC (95% CI)	AUC (95% CI)	AUC (95% CI)
Logistic regression	0.738 (0.682 to 0.793)	0.780 (0.712 to 0.849)	0.789 (0.743 to 0.835)
Naive bayes	0.729 (0.667 to 0.791)	0.780 (0.712 to 0.849)	0.771 (0.715 to 0.827)
K-nearest neighbors	0.607 (0.517 to 0.697)	0.643 (0.549 to 0.738)	0.646 (0.582 to 0.710)
Decision tree	0.567 (0.436 to 0.698)	0.671 (0.539 to 0.804)	0.671 (0.574 to 0.769)
Random forest	0.700 (0.640 to 0.760)	0.656 (0.574 to 0.739)	0.748 (0.692 to 0.804)
Support vector machine	0.586 (0.493 to 0.678)	0.442 (0.385 to 0.498)	0.520 (0.463 to 0.576)
Extreme gradient boosting	0.625 (0.509 to 0.741)	0.606 (0.478 to 0.734)	0.670 (0.570 to 0.769)
Light gradient boosting machine	0.672 (0.583 to 0.761)	0.721 (0.668 to 0.773)	0.735 (0.684 to 0.785)

Abbreviation: AUC, area under the receiver operating characteristic curve; CI, confidence interval.

Pre-Proof

Copyright *Chronic Obstructive Pulmonary Diseases: Journal of the COPD Foundation* ©2026
Published online November 23, 2026 https://doi.org/10.15326/jcopdf.2026.0850

Table S8. Baseline characteristics for the risk stratification in the combined model.

Characteristic	Training dataset (n=656)			Testing dataset (n=281)		
	Low risk (n=398)	High risk (n=258)	P Value	Low risk (n=161)	High risk (n=120)	P Value
Age — year	55.9±7.3	62.7±6.7	**<0.001**	56.0±6.49	61.8±6.93	**<0.001**
Male sex — no. (%)	136 (34.2)	252 (97.7)	**<0.001**	54 (33.5)	114 (95.0)	**<0.001**
Body mass index — kg/m^2	23.9±3.2	22.8±3.0	**<0.001**	23.8±3.1	22.7±3.2	**0.003**
Smoking status — no. (%)			**<0.001**			**<0.001**
Never smoked	307 (77.1)	47 (18.2)		121 (75.2)	26 (21.7)	
Former smoked	24 (6.0)	66 (25.6)		6 (3.7)	31 (25.8)	
Current smoked	67 (16.8)	145 (56.2)		34 (21.1)	63 (52.5)	
Smoking index — pack-year	9.3±22.4	34.2±32.5	**<0.001**	9.78±21.7	32.5±31.4	**<0.001**
Biomass exposure — no. (%)	144 (36.2)	85 (32.9)	0.396	59 (36.6)	33 (27.5)	0.106
Occupational history of dusts/gases/fumes — no. (%)	68 (17.1)	49 (19.0)	0.533	19 (11.8)	23 (19.2)	0.087
Family history of respiratory diseases — no. (%)	39 (9.8)	25 (9.7)	0.963	13 (8.1)	14 (11.7)	0.312
Respiratory symptoms — no. (%)						
Chronic cough	49 (12.3)	57 (22.1)	**<0.001**	24 (14.9)	26 (21.7)	0.143
Chronic sputum production	90 (22.6)	81 (31.4)	**0.012**	34 (21.1)	31 (25.8)	0.354
Dyspnea	67 (16.8)	59 (22.9)	0.055	46 (28.6)	22 (18.3)	**0.047**
Wheeze	17 (4.3)	14 (5.4)	0.496	15 (9.3)	10 (8.3)	0.775
mMRC score	0.19±0.46	0.27±0.54	**0.027**	0.32±0.53	0.23±0.55	0.198
CAT score	3.1±4.0	3.4±4.7	0.182	3.2±3.7	2.9±3.6	0.439
Spirometry						
Prebronchodilator FEV_1 — L	2.22±0.54	2.52±0.50	**<0.001**	2.19±0.55	2.57±0.52	**<0.001**
Postbronchodilator FEV_1 — L	2.30±0.54	2.60±0.50	**<0.001**	2.25±0.0.55	2.63±0.52	**<0.001**
Postbronchodilator FEV_1/FVC — %	81.0±5.5	75.9±4.3	**<0.001**	80.7±5.1	76.6±5.1	**<0.001**
Computed tomography						
Radscore	-2.89 (-3.39, -2.53)	-1.75 (-2.07, -1.27)	**<0.001**	-2.85 (-3.26, -2.46)	-1.77 (-2.05, -1.40)	**<0.001**

Data are presented as mean ± standard deviation, median (interquartile range), or n (%).

Abbreviation: CAT, chronic obstructive pulmonary disease assessment test; FEV_1, forced expiratory volume in 1 second; FVC, forced vital capacity; mMRC, the modified Medical Research Council.

Pre-Proof

Copyright *Chronic Obstructive Pulmonary Diseases: Journal of the COPD Foundation* ©2026
Published online November 23, 2026 https://doi.org/10.15326/jcopdf.2026.0850

Table S9. Association of the combined model risk stratification with spirometry-defined AO development and lung function decline using the lower limit of normal-defined AO in testing dataset.

Outcome	Parameter	Unadjusted		Adjusted*	
		Effect Estimate (95%CI)	P value	Effect Estimate (95%CI)	P value
AO development, n (%) †	**Percentage**				
Low risk	3 (1.7)	Reference		Reference	
High risk	65 (24.3)	18.99 (5.86 to 61.47)	**<0.001**	10.59 (2.52 to 44.56)	**0.001**
Annual decline in lung function	**Annual decline**				
Prebronchodilator FEV_1, mL/year					
Low risk	14±5	Reference		Reference	
High risk	37±4	23 (11 to 34)	**<0.001**	22 (10 to 34)	**<0.001**
Postbronchodilator FEV_1, mL/year					
Low risk	19±5	Reference		Reference	
High risk	37±4	18 (6 to 30)	**0.003**	20 (8 to 33)	**0.002**
Postbronchodilator FEV_1/FVC, %/year					
Low risk	-0.1±0.1	Reference		Reference	
High risk	0.6±0.1	0.7 (0.4 to 1.0)	**<0.001**	0.6 (0.3 to 0.9)	**<0.001**

Data are mean ± standard error or n (%).
Estimates as difference unless otherwise noted.
Abbreviations: AO, airflow obstruction; CI, confidence interval; FEV_1, forced expiratory volume in 1 s; FVC, forced vital capacity.
* The analysis was adjusted for age, sex, body mass index, smoking status, smoking index, biomass exposure, occupational history of dusts/gases/fumes, and family history of respiratory diseases. For the analysis of annual decline in lung function, the analysis was further adjusted for baseline corresponding spirometric values.
† Odds ratio.

Pre-Proof

Copyright *Chronic Obstructive Pulmonary Diseases: Journal of the COPD Foundation* ©2026
Published online November 23, 2026 https://doi.org/10.15326/jcopdf.2026.0850

Table S10. Association of the combined model risk stratification with spirometry-defined AO development and lung function decline in participants with postbronchodilator $FEV_1/FVC \geq 0.75$ in testing dataset.

Outcome	Parameter	Unadjusted		Adjusted*	
		Effect Estimate (95%CI)	P value	Effect Estimate (95%CI)	P value
AO development, n (%) †	**Percentage**				
Low risk	3 (2.2)	Reference		Reference	
High risk	4 (6.1)	2.88 (0.63 to 13.27)	0.174	1.35 (1.13 to 14.28)	0.801
Annual decline in lung function	**Annual decline**				
Prebronchodilator FEV_1, mL/year					
Low risk	11±5	Reference		Reference	
High risk	29±8	17 (-1 to 36)	0.069	15 (-5 to 36)	0.133
Postbronchodilator FEV_1, mL/year					
Low risk	14±6	Reference		Reference	
High risk	29±8	15 (-5 to 35)	0.131	18 (-4 to 39)	0.103
Postbronchodilator FEV_1/FVC, %/year					
Low risk	0.1±0.1	Reference		Reference	
High risk	0.7±0.2	0.6 (0.2 to 1.1)	**0.006**	0.5 (0.0 to 1.1)	**0.042**

Data are mean ± standard error or n (%).
Estimates as difference unless otherwise noted.
Abbreviations: AO, airflow obstruction; CI, confidence interval; FEV_1, forced expiratory volume in 1 s; FVC, forced vital capacity.
* The analysis was adjusted for age, sex, body mass index, smoking status, smoking index, biomass exposure, occupational history of dusts/gases/fumes, and family history of respiratory diseases. For the analysis of annual decline in lung function, the analysis was further adjusted for baseline corresponding spirometric values.
† Odds ratio.

Pre-Proof

Copyright *Chronic Obstructive Pulmonary Diseases: Journal of the COPD Foundation* ©2026
Published online November 23, 2026 https://doi.org/10.15326/jcopdf.2026.0850

Figure S1. Flow chart.

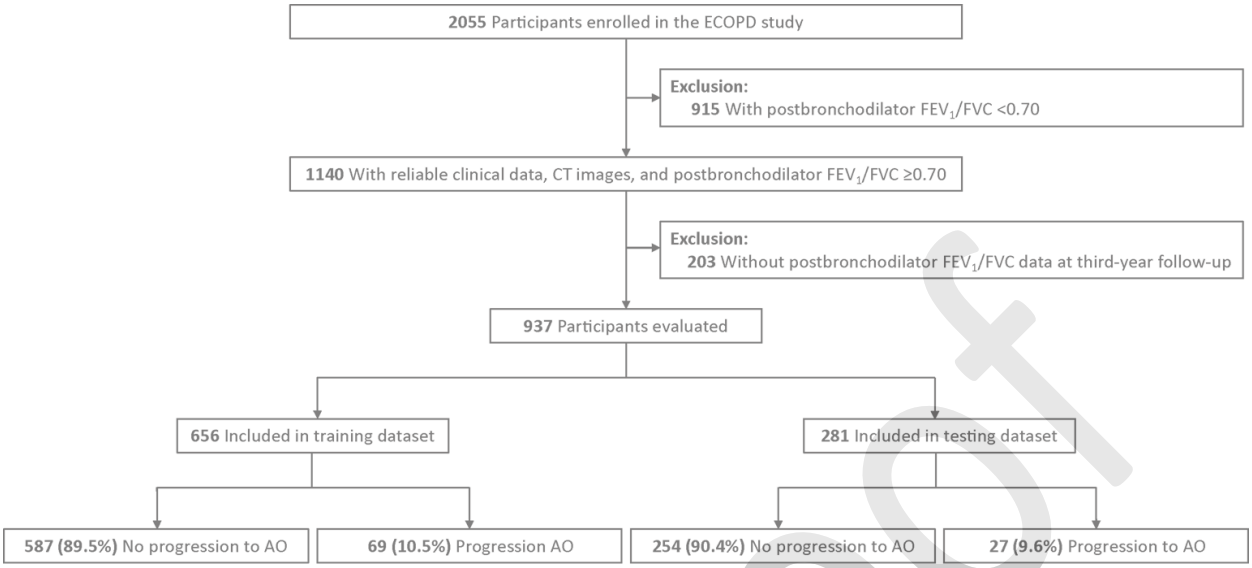

Abbreviations: AO, airflow obstruction; CT, computed tomography; FEV_1, forced expiratory volume in 1 second; FVC, forced vital capacity.

Figure S2. Calibration curves for the clinical, radiomic, and combined model.

Pre-Proof

Copyright *Chronic Obstructive Pulmonary Diseases: Journal of the COPD Foundation* ©2026
Published online November 23, 2026 https://doi.org/10.15326/jcopdf.2026.0850

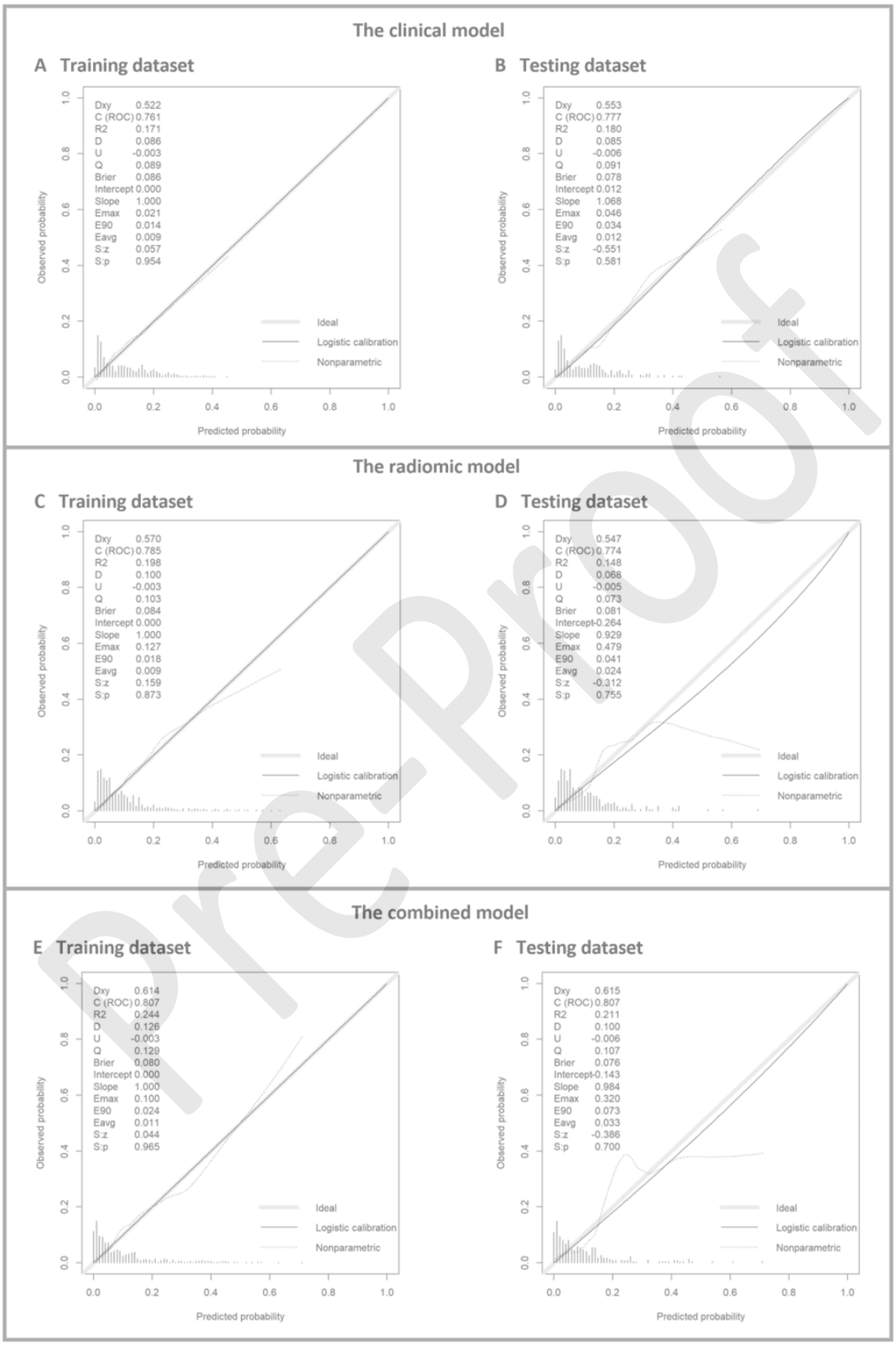

Pre-Proof

Copyright *Chronic Obstructive Pulmonary Diseases: Journal of the COPD Foundation* ©2026
Published online November 23, 2026 https://doi.org/10.15326/jcopdf.2026.0850

Figure S3. Decision curves for the clinical, radiomic, and combined model.

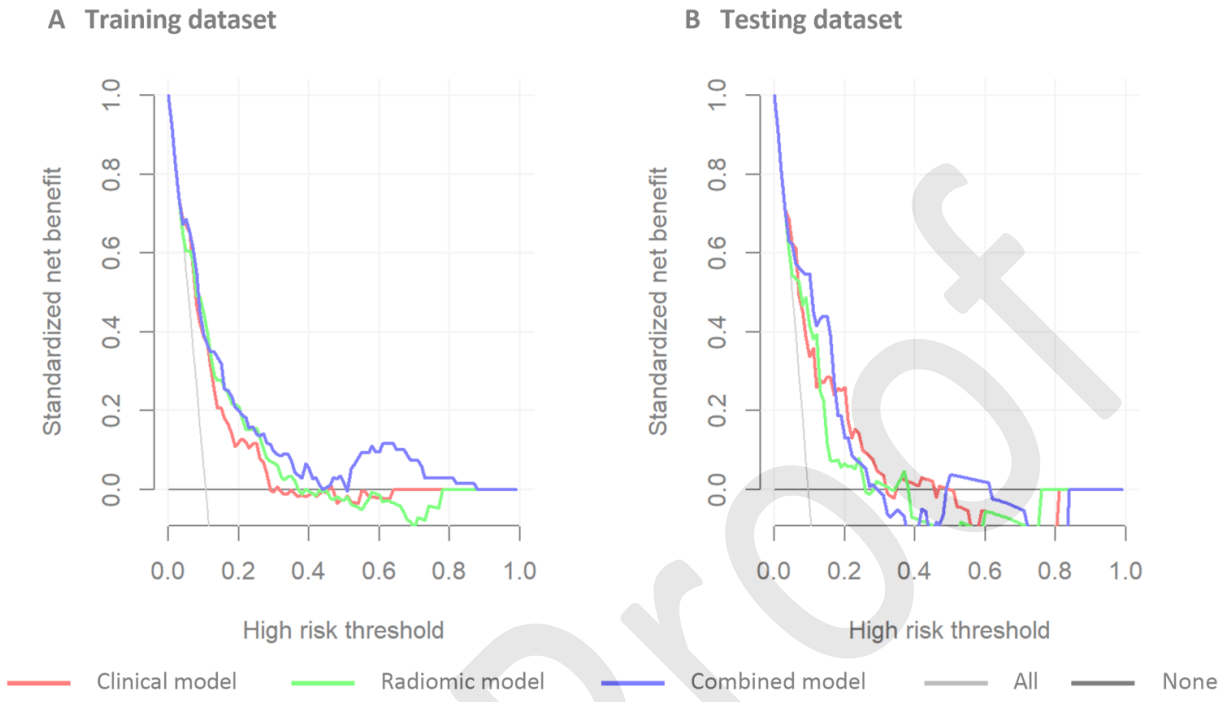

Figure S4. Airflow obstruction development risk stratified by spirometry-defined airflow obstruction risk stratification in the radiomic model.

Pre-Proof

Copyright *Chronic Obstructive Pulmonary Diseases: Journal of the COPD Foundation* ©2026
Published online November 23, 2026 https://doi.org/10.15326/jcopdf.2026.0850

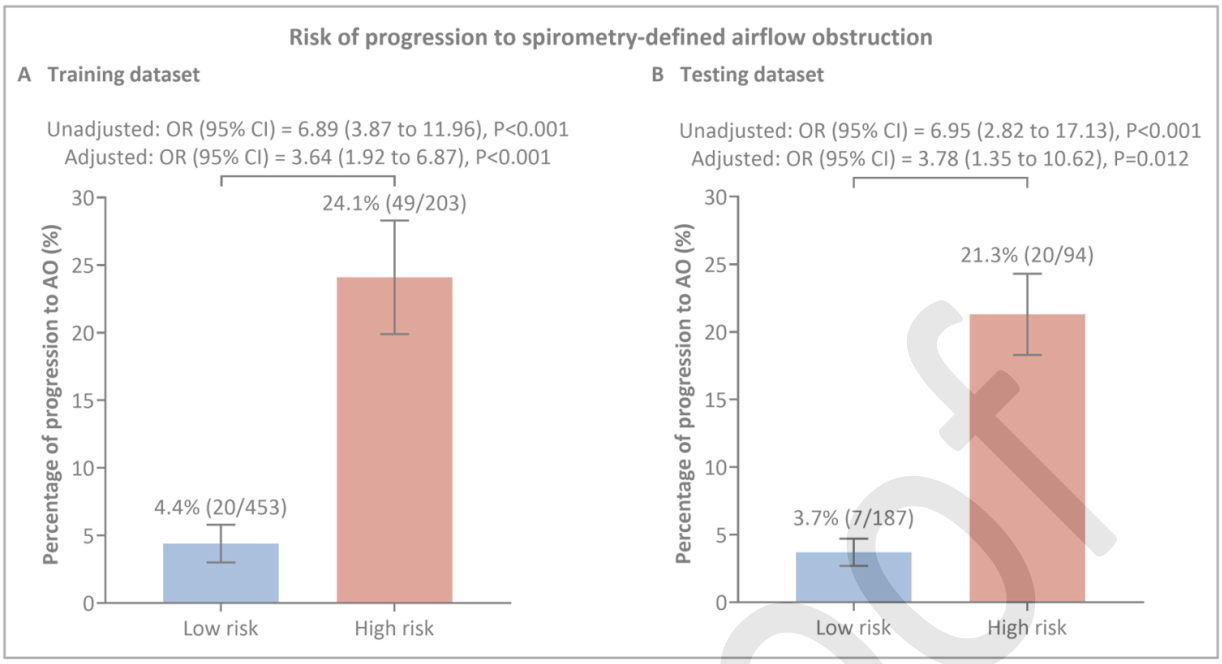

Data are presented as n (%).

Abbreviation: AO, airflow obstruction; CI, confidence interval; OR, odds ratio.

Figure S5. Airflow obstruction development risk stratified by spirometry-defined airflow obstruction risk stratification in the clinical model.

Pre-Proof

Copyright *Chronic Obstructive Pulmonary Diseases: Journal of the COPD Foundation* ©2026
Published online November 23, 2026 https://doi.org/10.15326/jcopdf.2026.0850

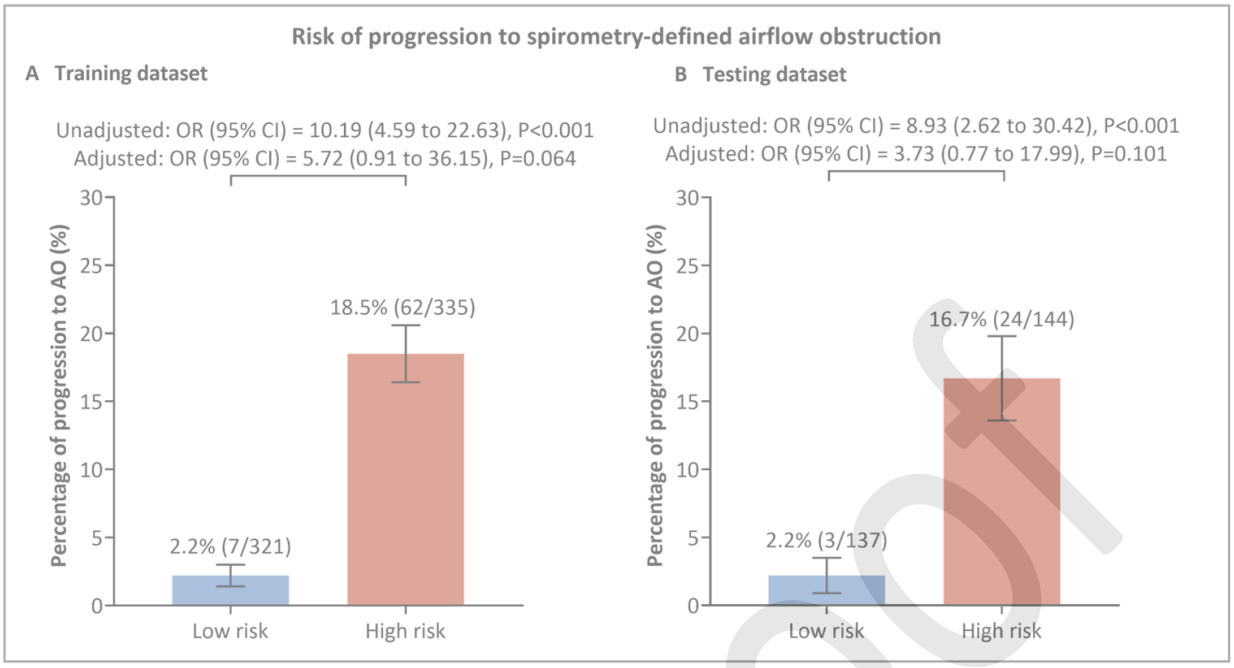

Data are presented as n (%).

Abbreviation: AO, airflow obstruction; CI, confidence interval; OR, odds ratio.

Figure S6. Annual decline in lung function stratified by spirometry-defined airflow obstruction risk stratification in the radiomic model.

Pre-Proof

Copyright *Chronic Obstructive Pulmonary Diseases: Journal of the COPD Foundation* ©2026
Published online November 23, 2026 https://doi.org/10.15326/jcopdf.2026.0850

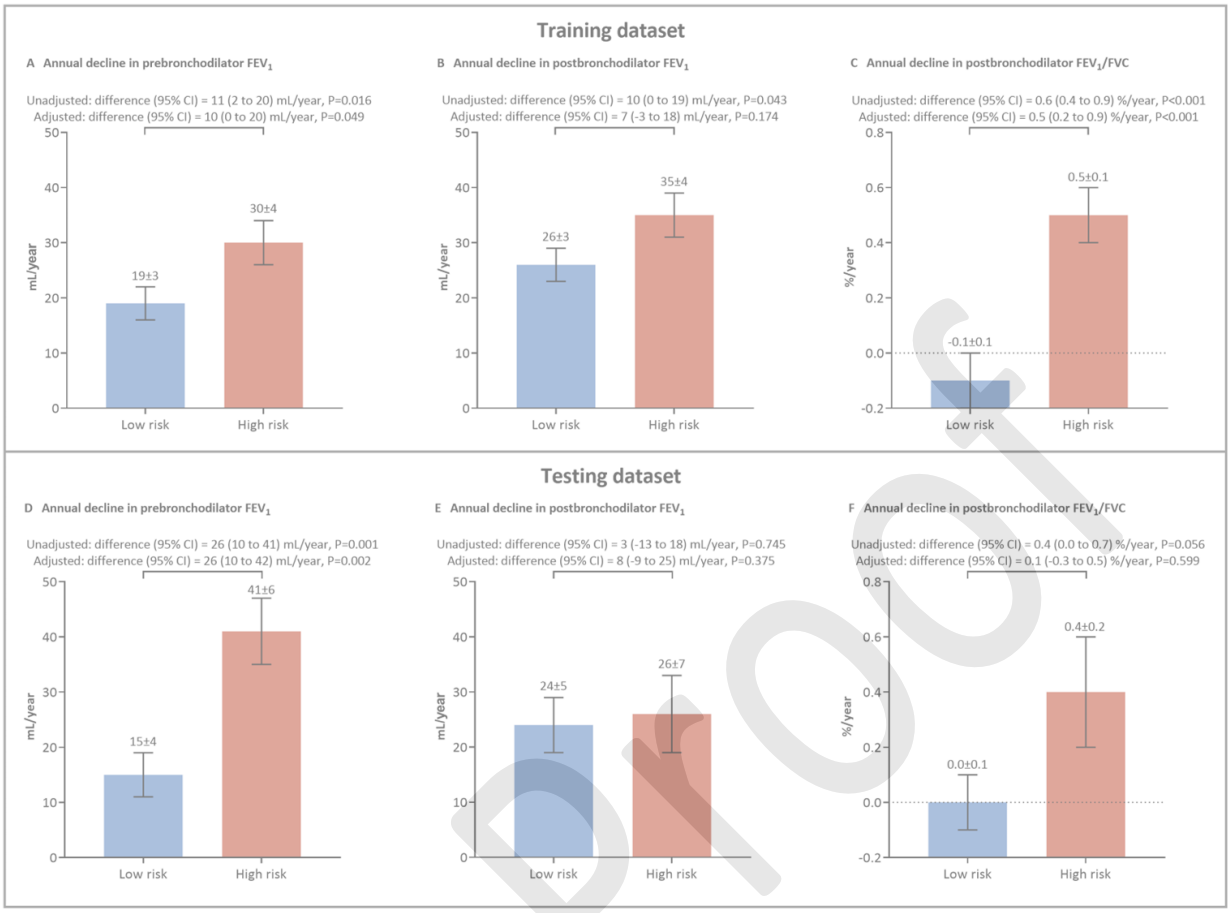

Data are presented as mean ± standard error.

Abbreviation: CI, confidence interval; FEV_1, forced expiratory volume in 1 second; FVC, forced vital capacity.

Figure S7. Annual decline in lung function stratified by spirometry-defined airflow obstruction risk stratification in the clinical model.

Pre-Proof

Copyright *Chronic Obstructive Pulmonary Diseases: Journal of the COPD Foundation* ©2026
Published online November 23, 2026 https://doi.org/10.15326/jcopdf.2026.0850

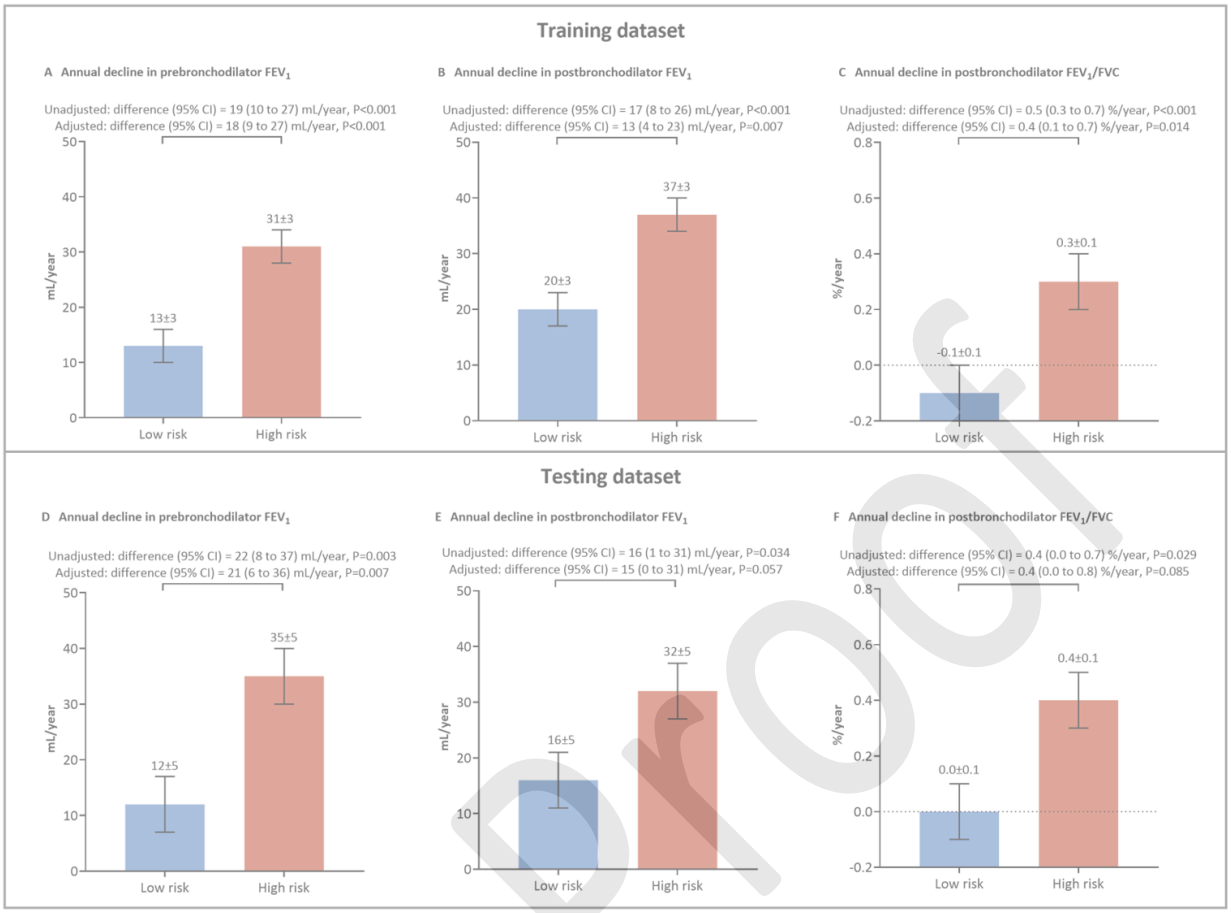

Data are presented as mean ± standard error.

Abbreviation: CI, confidence interval; FEV_1, forced expiratory volume in 1 second; FVC, forced vital capacity.

Pre-Proof

Copyright *Chronic Obstructive Pulmonary Diseases: Journal of the COPD Foundation* ©2026
Published online November 23, 2026 https://doi.org/10.15326/jcopdf.2026.0850